TG-1001
MAY 1968
Copy No 4

Technical Memorandum

A SPHERICAL FOCUSED BLAST DEVICE

by R. L. McCALLY

THE JOHNS HOPKINS UNIVERSITY • APPLIED PHYSICS LABORATORY

55

DISCLAIMER NOTICE

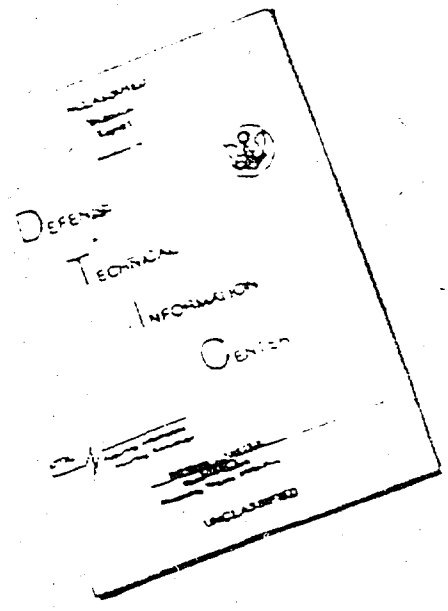

THIS DOCUMENT IS BEST QUALITY AVAILABLE. THE COPY FURNISHED TO DTIC CONTAINED A SIGNIFICANT NUMBER OF PAGES WHICH DO NOT REPRODUCE LEGIBLY.

This Document Contains Missing Page/s That Are Unavailable In The Original Document

THIS DOCUMENT CONTAINED BLANK PAGES THAT HAVE BEEN DELETED

REPRODUCED FROM BEST AVAILABLE COPY

TG-1001
MAY 1968

Technical Memorandum

A SPHERICAL FOCUSED BLAST DEVICE

by R. L. McCALLY

THE JOHNS HOPKINS UNIVERSITY • APPLIED PHYSICS LABORATORY
8621 Georgia Avenue, Silver Spring, Maryland 20910

Operating under Contract NOw 62-0604-c, Bureau of Naval Weapons, Department of the Navy

ABSTRACT

A spherical explosive device that, by selective multipoint initiation, concentrates its energy in a beam along any of several aiming axes is described. The aiming is accomplished by electronically selecting the proper group of detonators, thereby eliminating the necessity of physically aiming the charge which is required in all other focused blast devices. Once fired, these initiators cause a nearly cylindrical detonation wave, collapsing on the focusing axis, which forces the explosion products out along this axis.

Three small, 1/4 lb. C-4 spherical focused blast devices have been built and fired. The explosion products' velocity, shock wave velocity and peak pressure along the focusing axis were measured. These blast parameters were compared with similar ones measured for centrally initiated spheres, the purpose being to achieve a quantitative measure of the degree of focusing. The comparisons revealed that considerable gains over isotropic blast result from this focusing method. Furthermore, the focusing appears to be a far field effect in that the values of peak pressure and the shock velocity are nearly equal to those of the centrally initiated sphere in close but tend to fall off much less rapidly with distance.

Another result of interest is that the data obtained from the small, 1/4 lb., 2-inch diameter, centrally initiated spheres are in very good agreement with similar data scaled from much larger spheres.

ACKNOWLEDGEMENT

The author is grateful to Dr. F.K. Hill for suggesting this project and for the benefit of several helpful discussions. Also deserving of special thanks is Mr. E.N. Wallace, whose assistance during the experimental phase of this work was invaluable.

TABLE OF CONTENTS

LIST OF ILLUSTRATIONS

LIST OF ILLUSTRATIONS (Cont'd)

LIST OF TABLES

THE JOHNS HOPKINS UNIVERSITY
APPLIED PHYSICS LABORATORY
SILVER SPRING, MARYLAND

Introduction

Focused blast is the term applied to explosions that, by method of initiation, shape of explosive charge, or method of confinement, are directed in a beam or are uniformly distributed in a plane. For practical applications of focused blast, such as in missile ordnance, the explosive charge should have a symmetry that would permit producing the blast in any direction. This was recognized early at APL by W.H. Avery, who suggested that experiments with spherical charges having various arrangements of initiators be carried out at the New Mexico Institute of Mining and Technology, Socorro, New Mexico, to determine the degree of focusing that could be achieved. A patent application covering this device is on file. Later modifications of these ideas led to initiator arrangements which produced detonation waves that converged on the focusing axis and forced the explosive products out along this axis. Falcon Research, under subcontract to and in accordance with instructions from APL, measured the blast parameters around peripherally initiated charges of various geometries and compared the results with centrally initiated spheres of the same explosive. It was found that devices producing focused blast along an axis were more effective than those producing axisymmetric focused blast in a plane (Ref. 1). Both were more effective than centrally initiated spheres.

The spherical focused blast device described here is conceptually simple. Its focusing mechanism is identical to that of the flat, peripherally initiated disk which was the most effective device tested by Falcon Research (Ref. 1). In the peripherally initiated disk, the detonation waves collapsing cylindrically toward the center cause a strongly focused beam of explosion products along the axis perpendicular to the face of the disk. By properly arranging a number of detonators on the surface of a sphere and firing them at the correct time, a series of detonation waves collapsing on a polar axis, and, therefore, focusing the products along the polar axis, can be produced.

Consider a sphere of explosive having a radius, a, and twelve (12) initiation points arranged as shown in Figure 1. The four lying in the equatorial plane, i.e., the x-y plane, are to be initiated first, at $t = 0$, and the eight points lying in the two parallel planes are to be initiated later at $t = t_d$. The delay time, t_d, is the time required for the detonation wave from point A, initiated at $t = 0$, to reach the line B-B'. Thus.

$$t_d = \frac{a\ (1 - \sin \varphi)}{D} \qquad (1)$$

where D is the detonation velocity of the explosive and φ is the angle shown in Figure 1. It is expected that the collapsing detonation waves, so produced, will focus the explosion products along the z axis.

The device just described has only a single focusing axis. By adding more initiation points, the beam can be aimed along any desired axis simply by firing the proper combination of detonators. The method of locating these initiation points is discussed in the appendix.

Experimental Methods

A. The Initiation System:

Before the spherical focused blast device could be tested, it was necessary to develop a suitable initiation system. The maximum explosive weight of 1/2 pound allowed for testing here at APL placed severe constraints on the initiators. A 1/2 pound sphere of C-4, the planned explosive, is only about 2.5 inches in diameter; thus the initiators must be extremely small if they are to approximate points, yet they must also be very powerful to initiate the explosive with a small induction distance. Furthermore, for any reasonable choice of the angle φ (Eq. 1), the delay time is of the order of 1 μ s, so the initiators must function with timing errors no greater than 0.10 μ s. Available electrical detonators capable of this accuracy (the AEC SE-1 for example) are too large for the 2.5 inch sphere. Therefore, it was decided to develop an

initiating system consisting of twelve pieces of Detacord*, initiated simultaneously, with timing controlled by cord length.

Tests were necessary to determine if Detacord could reliably initiate C-4 and if it had sufficient uniformity to reproduce initiation times with the required accuracy. For initial testing, a simple method was devised which required a minimum of preparation and no instrumentation. Twenty grams of C-4 were held in a small bakelite cylinder which was placed, end on, on a 1" thick steel witness block (Figure 2). Two Detacord initiators were placed on opposite sides of the cylinder and embedded one-cord diameter in the C-4.

A detonation wave moving through the C-4 makes a deep dent in the witness block, and if two detonation waves meet they make a sharply defined meeting line in the block. Such a meeting line from one of the tests is illustrated in Figure 3. Since the detonation velocity of C-4 is known, (8.04 mm/μsec) initiation delays caused by the two cords can be calculated from the position of the meeting line.

These initial tests indicated that:

1. 0.190 inch diameter Detacord will reliably initiate Composition C-4.
2. Detacord has sufficient uniformity to produce the required initiation accuracy.
3. Initiating several cords simultaneously is difficult.
4. Controlling the length of the cords to the required accuracy is a major problem.

Originally it had been planned to use 0.110 inch diameter Detacord because it would more closely approximate a point initiator; however, tests showed that it would not initiate C-4. It was suggested that if the end of the cord was hollowed out, the shaped charge effect might be sufficient to initiate C-4. Subsequent experiments indicated considerable enhancement, as evidenced by deep dents in steel witness blocks, but the 0.110 inch cord still would not initiate C-4. Therefore, it was necessary to use 0.190 inch Detacord.

---

* Trade-name J.E. Dupont

The cords must be cut very precisely; since the detonation velocity in the cord is 7.00 mm/μ s, an error of only 0.7 mm in length corresponds to a timing error of 0.10 μ s. This problem is compounded by the rubbery nature of Detacord. Great care must be exercised in the cutting and subsequent handling of the cords so that they are not stretched or otherwise deformed. A simple jig, which rigidly supports the Detacord during cutting, was constructed from two blocks of lucite machined to the proper length. A groove is milled in one of the blocks to accommodate the Detacord, the other block clamps the cord firmly in position while it is cut at each end with a razor blade.

The problem of simultaneously initiating the twelve pieces of Detacord was solved by placing them on the periphery of a 2-inch diameter disk of Detasheet. The Detasheet disk was then initiated at its center by an E-106 cap. A drawing of this system is shown in Figure 4. High speed photographs (1.0×10^6 frames/sec) showed that all the cords were initiated simultaneously within 1.0 μ s (the interframe time).

The entire initiating system was assembled and tested. Photographs indicated that the detonation waves arrived at the end of the cords simultaneously, within the measuring error of the experiment (0.10 μ sec) which depends entirely on how accurately the distance of the waves from the end of the cord at a particular time could be measured on the film. This result means that the initiation system employing pieces of Detacord was sufficiently accurate to use for the preliminary sphere tests.

A small, powerful electrical detonator was required to initiate the centrally initiated spheres used for the control experiments. Timing was no problem in these experiments. The EX-7 miniature detonator (manufactured by the Hercules Powder Company, Port Ewen, New York) meets these requirements. These are sufficiently powerful and quite small (0.410" x 0.188" diameter at the firing end).

B. Construction of the Spheres:

Two-inch diameter C-4 spheres, weighing approximately 1/4 pound, were used for the experiments. Table I shows the actual explosive weights, including the Detacord initiating system, for each test. The spheres were made by hand packing explosive into 2.0 inches I.D. cast epoxy shells having .20 inch walls. These shells serve both as spherical molds and as collars for

accurately locating and holding the initiating cords in position. Figure 5 is a photograph of one of the epoxy shells with holes drilled to accommodate the initiators. The angle φ (Eq. 1) was chosen as 43° 9' to make the delay exactly 1.0 μ s. The epoxy shell, filled with explosive, was suspended in a framework of 1/16 inch lucite sheets which supported the pieces of Detacord in the initiating system. A spherical focused blast device, ready for testing, is shown in Figure 6.

The centrally initiated spheres for the control experiments were made in halves, each half being made by molding C-4 in one of the cast epoxy shells which had been lined with nylon net to facilitate removal of the charge. The EX-7 detonator was inserted by making a suitable dent in each hemisphere. Assembly was completed by tightly taping the sections together. During the test the sphere was suspended in a small nylon net or cloth bag.

Instrumentation

High-speed photographs of the expanding explosion products' cloud were taken with a 16 mm Fastax camera. The speed of the camera was determined accurately from timing light marks on the edge of the film. The timing light was driven by an audio oscillator whose frequency was continuously monitored with an electronic counter. By including an appropriate grid in the photographs, the explosion products' position could be determined as a function of time and their velocity could be obtained by graphically differentiating these data.

Attempts were made to measure the pressure, with piezoelectric transducers, at a number of positions along the focusing axis. Each transducer was connected to a Tektronix 565 oscilloscope through Kistler 566 charge amplifiers. Borrowing a technique from aerodynamics, the gauges were mounted in a flat steel plate, 2' x 4' x 1/2", which had a 2° wedge mounted on the front. The plate was held vertically and aligned along the focusing axis of the sphere. The pressure measured in this manner is the static pressure.

Time of arrival data for the shock wave at six distances were also obtained,using piezoelectric transducers, for most of the tests. (The six gauges include the two transducers mounted in the steel plate). For the

centrally initiated sphere tests, the gauges were distributed around the sphere while they were placed essentially along the focusing axis for the focused sphere test. Because of the small scale of the test, they could not be placed directly on the axis one after another inasmuch as the flow is disturbed behind the gauge. Therefore, care was taken to position each gauge so that it would not interfere with others behind it. Figure 7 shows a schematic of the gauge positions. The shock velocity can be deduced from these data and the pressure distribution calculated from the measured shock velocity using the normal shock relation for a perfect gas.

$$\frac{P}{P_o} = 1 + \frac{2\gamma}{\gamma + 1} (M^2 - 1) \qquad (2)$$

where P = absolute pressure

P_o = ambient pressure

M = shock Mach number = v/c

γ = 1.4 for air

c = local sound velocity

The ideal gas assumption is certainly justified; because, for the low Mach numbers encountered, the real gas correction is negligible (Ref. 2).

Experimental Results

A. Centrally Initiated Spheres:

Two 2.0 inches in diameter, centrally initiated, C-4 spheres were fired to serve as a control for the focused blast experiments. Gas cloud shape and velocity and shock velocity were measured and attempts were made to measure the pressure at two distances from the spheres. Table II shows the locations of the six transducers. Gauges P_4 and P_5 were mounted in the steel plate to measure static pressure. Gauges P_1 and P_4 were interchanged for the second firing because the sensitivity of the Kistler 605B was found to be too low to measure the pressure at the P_4 location.

Traces from successive frames of the Fastax films of each test are shown in Figure 8. The explosions of both spheres are uniform except for minor localized disturbances on the expanding fronts.

Time-of-arrival data for both spheres are plotted in Figure 9; also shown, are the positions of the explosion products determined from the photographs. It was necessary to shift these points by a constant time to make them have the same zero as the time-of-arrival data because the actual zero time of the event occurred between frames of the film. The data from both spheres are in close agreement; so single curves are fitted through the points.

The shock wave and explosion products' velocities were determined from the distance-time curves and are shown in Figure 10.

Table III shows the peak pressures measured at locations P_4 and P_5. Pressure-time histories were not obtained because of severe gauge ringing and apparent thermal effects, evidenced by the drift of the scope trace from its zero level. As mentioned previously, no pressure was measured at the P_4 location for the first test because the gauge was too insensitive.

The pressure distribution was calculated from the shock velocity using Equation 2 with P_o = 14.7 psi and c = 1100 ft/sec. These pressures are plotted in Figure 11 along with the measured pressures from Table III. The calculated and measured pressures are not in good agreement. In fact, the measured pressures are each almost exactly half the corresponding calculated ones. It is felt that this relationship is fortuitous, and that the disagreement is an indication of damped gauge response caused by the protective coating of silicone grease placed on the transducer face; especially since the calculated pressures are in good agreement with scaled data from larger charges (See Discussion).

B. Focused Blast Results:

Three spherical focused blast devices were built and fired. No data, except photographs, were obtained from the first firing; however, these looked promising enough to continue this program.

Figure 12 shows traces from the photographs of both the second and the third tests. A considerable degree of gas cloud focusing is evident in both of these tests; however, the focused beam is directed upward, 12^{o} in the second test and 13.5^{o} in the third, from the planned axis. Presently, it is felt that the large amount of additional explosive in the initiation system causes this deflection.

In the second test, three pressure transducers were mounted in the steel plate in an attempt to make pressure measurements on the focusing axis. Table IV shows the location and types of these gauges. Time-of-arrival data were taken only for the third test and the instrumentation was identical to that used for the second centrally initiated sphere test (See Table II).

The positions of the explosion products, for the second test, as functions of time are plotted in Figure 13.

The shock wave time-of-arrival data and the position of the explosion products of the third test are shown in Figure 14. The time-of-arrival data have been corrected to compensate for the delay in the initiating system. This was necessary because the scope recording the data is triggered at the same time as the E106 cap receives its firing pulse, while the actual zero time of the event is when the sphere is initiated. The E106 cap has a typical delay of 30 μ s and the delay in the Detasheet disk and 12.0 inch lengths of Detacord are computed from their respective detonation velocities to be 47.1 μ s, making the total correction 77.1 μ s (.077 ms). The explosion products' position curve was shifted, exactly as in the centrally initiated sphere tests, to make it have the same time zero as the time-of-arrival data. The time-of-arrival data obtained are coincident with the gas cloud points, indicating that the shock wave had not yet separated from the rapidly moving explosion products' front. Two of the gauges, P_5 and P_6, failed to operate; so the shock wave separation was not observed. Close examination of the films indicated that neither gauge was struck by the direct wave because of its upward direction.

The distance-time curves for each test were graphically differentiated

to determine the shock wave and explosion products' velocities, which are plotted as a function of distance from the center of the sphere in Figure 15. The gas cloud velocities measured for the two spheres are slightly different, with the third sphere's products' front having a higher velocity than that of the second. These measurements are consistent with the appearance of the two blasts in that the beam of the third device appears narrower than that of the second. The general shape, however, of the velocity curves is nearly identical, indicating that the functional dependence of velocity on distance is the same in both tests. Both curves have two inflection points; the second derivative, d^2v_p/dr^2, shifting from positive to negative and back to positive again. In the third test, the shock wave and explosion products' velocities are equal up to the first inflection point. It is postulated here, without proof, that the first inflection point is associated with the separation of the shock wave from the products' front.

The pressure measurements were not entirely successful for either the second or the third test. In the second test, gauges P_2 and P_3, located 3.5 and 5.0 feet from the center of the sphere, failed to operate and the trace of gauge P_1 was almost entirely obscured by ringing; but, an approximate peak overpressure of 90 psi was measured. In test three, gauges P_5 and P_6 didn't function but gauge P_4 had the best, i.e., least noisy, trace recorded during the entire test series; a peak overpressure of 120 psi was measured. Again, the pressure was calculated from the measured shock velocity of test three using Eq. 2 with P_o = 14.7 psi and c = 1100 ft/sec. These pressures and the measured pressure at 2.5 feet are plotted in Figure 16. The measured pressure is only one-third of the calculated pressure at the same distance (120 psi vs 360 psi), which is worse agreement than was obtained for the centrally initiated sphere tests where the measured pressure was half the calculated pressure. Part of this discrepancy can again be attributed to damped gauge response, but some of the deviation may have been caused by the fact that the gauge was off the direct focusing axis because of the beam's upward motion. If true, this would explain why the difference between measured and calculated pressures is greater in the focused than in the isotropic sphere tests.

Discussion

Figure 12, showing the shape of the explosion products' cloud as it expands from the spherical focused blast device, clearly shows that a high degree of focusing was achieved with the proposed multipoint initiating system. The shape of the gas cloud, however, is only a qualitative indication of focusing. A quantitative measure is needed. The isotropic blast from a centrally initiated sphere of the same weight and material provides an ideal lower limit of no focusing for direct comparisons. Such comparisons are made in Figures 17 and 18, where the shock wave and explosion products' velocities and the peak overpressure obtained from the centrally initiated sphere and focused blast tests are shown together. The gains achieved by focusing are considerable. For example.

1. The gas cloud velocity has fallen to 1500 ft/sec at only 1.95 feet from the isotropic sphere. This same velocity occurs at 4.0 ft from the focused sphere.
2. At 2.5 ft the shock velocity is 2400 ft/sec for the center initiated sphere and 5200 ft/sec for the focused device and the pressure of the focused sphere is more than five times greater (360 psig vs. 65 psig).

Even more interesting is that the focusing effect increases with distance from the blast center. This is illustrated in Figure 19, where the ratio of the absolute pressure obtained from the focused sphere to that from the isotropic sphere is plotted as a function of distance. This curve will have a maximum when the wave from the centrally initiated sphere drops to sonic velocity and then the ratio will decrease to unity. This result is surprising, because intuitively one might have expected the pressure ratio to be a monotonically decreasing function of distance.

It is of considerable interest to know how the spherical focused blast device compares to other types of focused charges. Falcon Research and Development Corp., under subcontract to APL, fired charges of several types to investigate their focusing characteristics (Ref. 1). Included among these were:

1. Three types of peripherally initiated disks (all Comp. B, weighing 20 lbs.), a flat one, a convex-concave one, and a double convex disk.
2. Confined and unconfined, 60 lbs. simultaneous end initiated cylinders - also Comp. B.
3. Multipoint, side initiated and centrally initiated, 20 lbs. Comp. B spheres.

F.K. Hill, APL, has plotted the peak excess pressure obtained from each of these charges as a function of the scaled distance $Z = (R/W^{1/3})\ P_o^{1/3}$; i.e., the pressures have been referenced to 1 lb. charges fired at sea level. His plot is shown in Figure 20, where the results of the spherical focused blast tests have been added for comparison. This was done in full recognition of the fact that Sachs' cube-root scaling law applies only to isotropic blasts such as from centrally initiated spheres and its use here is probably invalid.

Having obtained what appear to be good data for small centrally initiated spheres, it is of considerable interest to examine the validity of scaling similar data, obtained for much larger spheres, down to this size. The type of scaling of interest is that used in the previous paragraph, namely, if a sphere of weight W_1 causes a pressure P at a distance R_1, then another sphere, having weight W_2, will produce the same pressure at another distance R_2, given by

$$R_2 = \left(\frac{W_2}{W_1}\right)^{1/3} R_1 \qquad (3)$$

if the ambient pressure is the same for both tests. No data from large C-4 spheres could be found for comparison with the 1/4 lb. C-4 sphere data; however, data from 20 lbs. 50/50 Pentolite and Comp. B spheres were available (Refs. 1 and 3). If two explosives have equal values of their energy of detonation and adiabatic exponent, they produce identical effects. Detonation velocity is an equally valid comparison parameter since the three quantities are related by

$$E = \frac{D^2}{2(\gamma^2 - 1)} \qquad (4)$$

where E, D and γ are the energy of detonation, detonation velocity and adiabatic exponent respectively. The values of these parameters for 50/50 Pentolite, Comp. B, RDX and C-4 are tabulated in Table V. RDX is included because of incomplete C-4 data. C-4, which is a mixture of 91% RDX and 9% solvent-plasticizer, should act very much like pure RDX. The fact that Pentolite and Comp. B have lower energies of detonation and detonation velocities than RDX (or C-4) indicates that they should produce slightly lower shock velocities and pressures. The scaled data are included in Figures 10 and 11 and are seen to be in good agreement with the 1/4 lb, C-4 data, but, as expected, slightly lower. The average deviation between scaled and measured pressure is only about 10%, thus, when the differences in explosives are considered, it appears that blast pressures from centrally initiated spheres can be scaled to very small charges with little error.

The work described here is of a preliminary nature. A spherical focused blast device, employing selective multipoint initiation, capable of firing in any chosen direction by electronically choosing the proper group of initiators, has been tested in small scale experiments and appears to be highly effective. More complete data are required to accurately assess its effectiveness with respect to other types of focused blast. More complete pressure data, including pressure-time histories both on and off axis are needed. The pressure-time history is required to calculate the impulse, which is one of the main parameters used for predicting the damage potential against various targets. The off axis pressure is needed to determine the focused beam width which is necessary for deciding on the number of focusing axes required to provide the greatest effectiveness. At the present time, however, comparisons of pressure and impulse between different types of focused blast charges can only be made for charges having the same weight and fired under the same ambient conditions. It is even impossible to predict the behavior of two charges having identical geometries but having different weights and possibly fired under different ambient conditions. This is one of the worst deficiencies of focused blast technology; it is not yet well enough understood, nor has enough information been collected, to develop simple methods of predicting blast effects such as the scaling laws that apply to isotropic blasts.

APPENDIX I

Initiation System for Multi-directional Spherical Focused Blast Device

A practical spherical focused blast warhead must be capable of firing along any of several possible axes. The proper firing axis would be determined by the relative attitude between the missile and target at intercept and the appropriate group of detonators triggered electronically. The entire system, being electronically controlled and fired, would have a nearly instantaneous response.

In the following, a systematic method of locating the initiation points will be developed. It will be shown that the points occur in pairs which are reflections of each other through the center of the sphere. These paired points are always fired simultaneously and certain of them are always delayed, which simplifies the switching network required to choose them.

Consider a sphere of radius a, having nine firing axes, i.e., axes (1 - 9), arranged as in Figure 21. The numbers 10 - 13 are for later reference. Let the center of this sphere be at the origin of the xyz coordinate system and let the z axis coincide with the missile axis. If the z axis were the firing axis, the twelve initiation points would be located at (referring to Figs. 1 & 21)

$$\bar{x} = a\begin{pmatrix}\pm 1\\ 0\\ 0\end{pmatrix}, \quad a\begin{pmatrix}0\\ \pm 1\\ 0\end{pmatrix}, \quad \frac{a\sqrt{2}}{2}\begin{pmatrix}\pm 1\\ 0\\ 1\end{pmatrix}, \tag{A-1}$$

$$\frac{a\sqrt{2}}{2}\begin{pmatrix}\pm 1\\ 0\\ -1\end{pmatrix}, \quad \frac{a\sqrt{2}}{2}\begin{pmatrix}0\\ \pm 1\\ 1\end{pmatrix} \quad \text{and} \quad \frac{a\sqrt{2}}{2}\begin{pmatrix}0\\ \pm 1\\ -1\end{pmatrix}$$

where column matrix notation is used for the coordinates. Now let z' in the x'y'z' system be any other firing axis. The initiation points for this axis will have the same coordinates in the x'y'z' system as the initiation points for the z axis in the xyz system. It is desired, then, to find the coordinates of these points in the xyz system. Now the x'y'z' axis can be formed by rotating the xyz axis and the most systematic method of performing this rotation is the method of Euler angles (Ref. 6). In this approach,

the rotation is decomposed into three separate ones as in Figure 22.

1. The xyz system is rotated counterclockwise about the z axis through an angle φ, resulting in the intermediate $\xi\eta\zeta$ system.
2. The $\xi\eta\zeta$ system is then rotated counterclockwise, through an angle θ, about the ξ axis to produce the $\xi'\eta'\zeta'$ system.
3. Finally, the $\xi'\eta'\zeta'$ system is rotated counterclockwise about the ζ axis through angle ψ, resulting in the x'y'z' system.

Thus in matrix notation

$$\dot{x}' = A\,\dot{x} \tag{A2}$$

where $\dot{x}' = \begin{pmatrix} x' \\ y' \\ z' \end{pmatrix}$ and $\dot{x} = \begin{pmatrix} x \\ y \\ z \end{pmatrix}$.

and the matrix A is the product of the three separate rotation matrices B, C and D where,

$$B = \begin{pmatrix} \cos\psi & \sin\psi & 0 \\ -\sin\psi & \cos\psi & 0 \\ 0 & 0 & 1 \end{pmatrix} \tag{A3}$$

$$C = \begin{pmatrix} 1 & 0 & 0 \\ 0 & \cos\theta & \sin\theta \\ 0 & -\sin\theta & \cos\theta \end{pmatrix} \tag{A4}$$

$$\text{and} \quad D = \begin{pmatrix} \cos\varphi & \sin\varphi & 0 \\ -\sin\varphi & \cos\varphi & 0 \\ 0 & 0 & 1 \end{pmatrix} \tag{A5}$$

Table VI shows the Euler angles φ, θ and ψ for the firing axes indicated in Figure 21. ψ is zero for all of these, so B reduces to the identity matrix. Thus A = CD or

$$A = \begin{pmatrix} \cos\varphi & \sin\varphi & 0 \\ -\sin\varphi\cos\theta & \cos\varphi\cos\theta & \sin\theta \\ \sin\varphi\sin\theta & -\cos\varphi\sin\theta & \cos\theta \end{pmatrix} \tag{A6}$$

Now recall that $\vec{x}'$ is known and $\vec{x}$ is sought; therefore,

$$\vec{x} = A^{-1}\vec{x}', \tag{A7}$$

but A is an orthagonal matrix; so, its inverse is equal to its transpose; i.e., $A^{-1} = A^{T}$.

Therefore,

$$\vec{x} = A^{T}\vec{x}', \tag{A8}$$

where

$$A^{T} = \begin{pmatrix} \cos\varphi & -\sin\varphi\cos\theta & \sin\varphi\sin\theta \\ \sin\varphi & \cos\varphi\cos\theta & -\cos\varphi\sin\theta \\ 0 & \sin\theta & \cos\theta \end{pmatrix} \tag{A9}$$

The value of A^{T} for each firing axis is found by substituting in the values of φ and θ that appear in Table VI. The resulting transformation matrices for each of the nine firing axes are tabulated in Table VII. By using these matrices and the coordinates of the firing points in the primed system given in Eq.(A1), the positions of the initiation points in the xyz system can be found from Eq. (A8). These are collected in Table VIII. Table IX gives the initiation points and their firing order for each firing axis.

By careful examination of the initiation points in Table VIII, it is seen that they are comprised of twenty-one pairs of points, and that the pairs are reflections of each other through the origin. Furthermore, Table IX shows that the pairs are always fired simultaneously; the ones on the firing axes; i.e., those numbered 1 through 9, being fired either with or without delay and the others; viz., the ones numbered 10 through 13 and the lettered ones, always being delayed.

A practical device would consist of twenty-one high voltage pulse circuits, each connected to two exploding bridgewire detonators. These pulsers would be tied to the missile fuze by a switching network of diodes that would, upon receiving the proper signal, select and trigger the proper group of modules to direct the blast at the target.

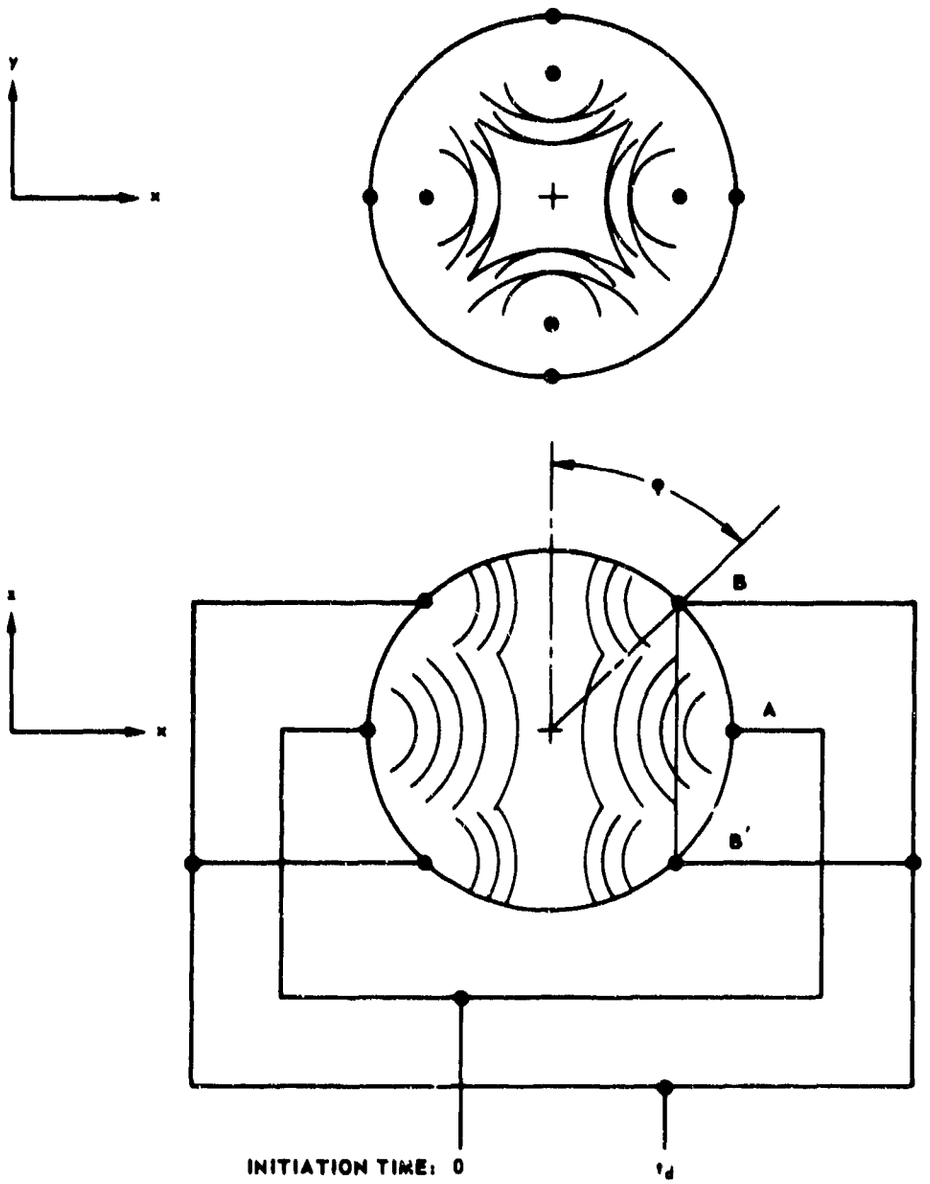

Fig. 1 LOCATION OF INITIATION POINTS FOR SPHERICAL FOCUSED BLAST DEVICE

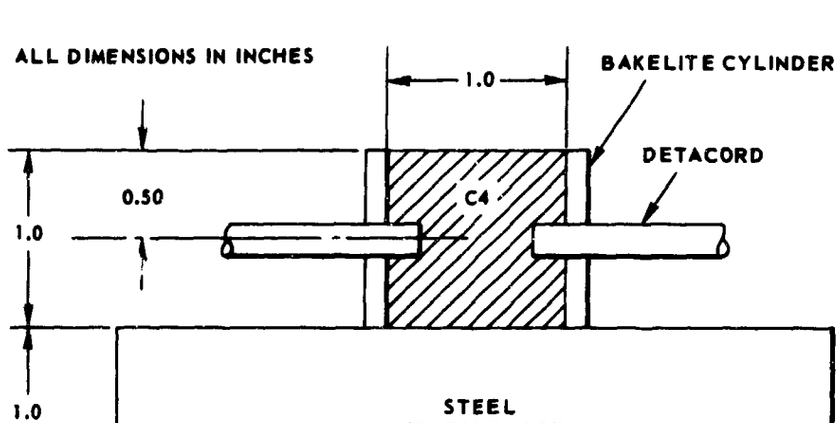

Fig. 2 APPARATUS FOR DETERMINING INITIATION SIMULTANEITY

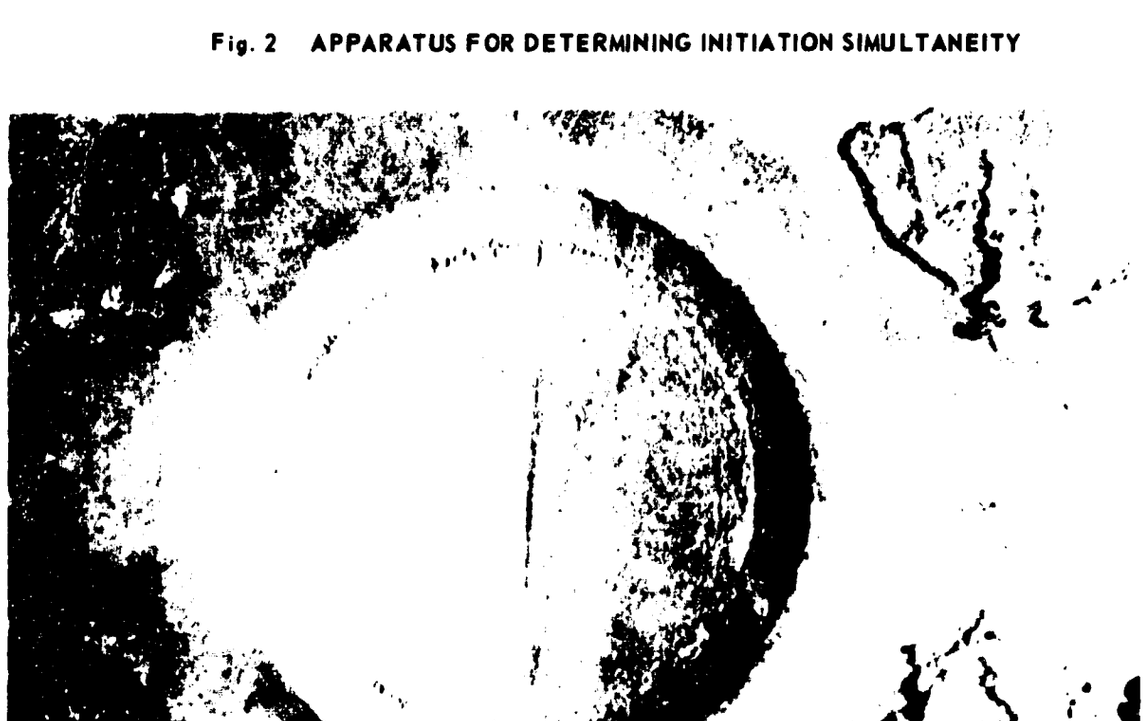

Fig. 3 WITNESS BLOCK, SHOWING MEETING LINE

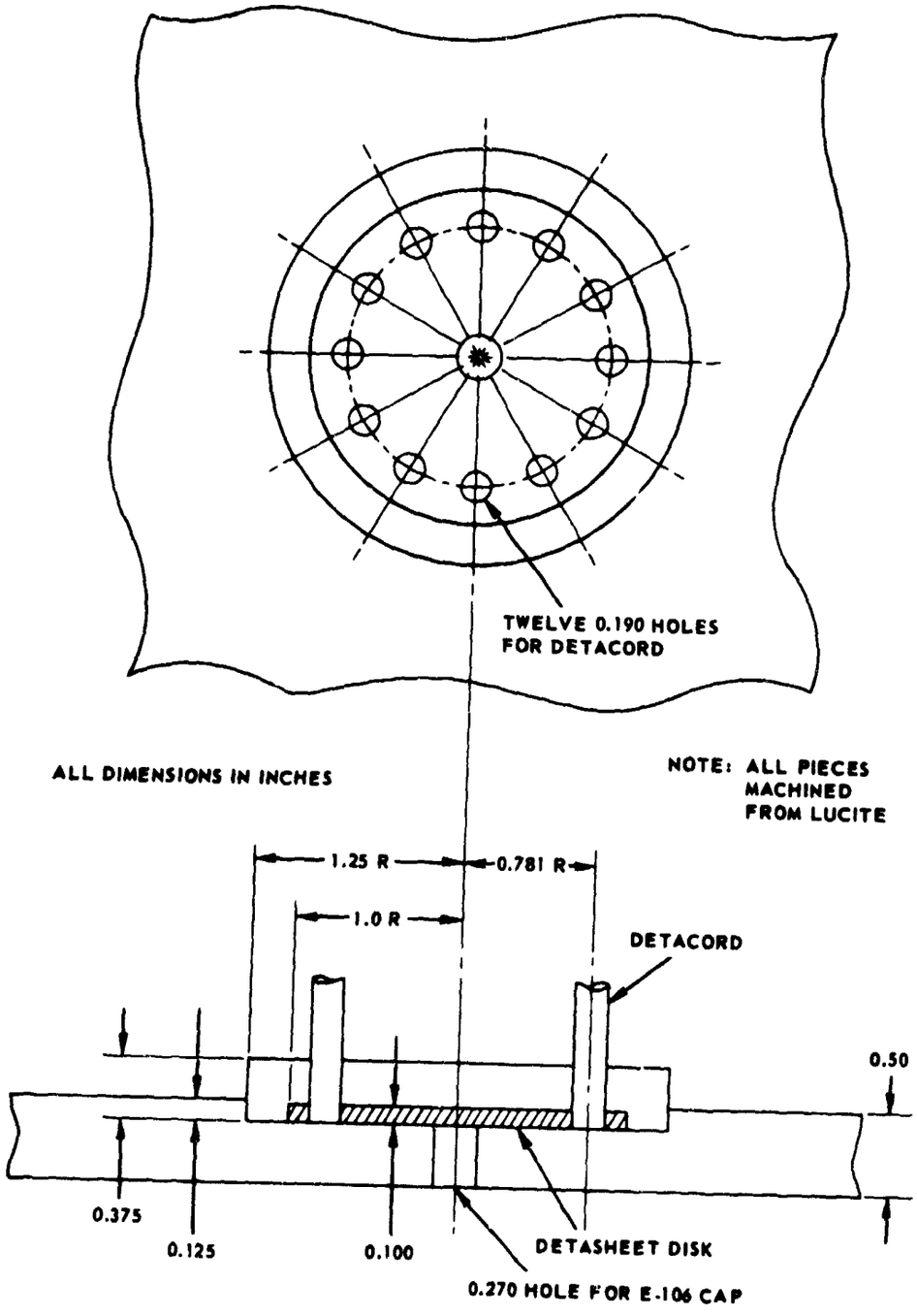

Fig. 4 DETAILS OF INITIATION SYSTEM

Fig. 5 SPHERICAL EPOXY SHELL

NOTE: THE LENGTHS OF DETACORD ARE SIMULATED BY PLASTIC SPAGHETTI TUBING

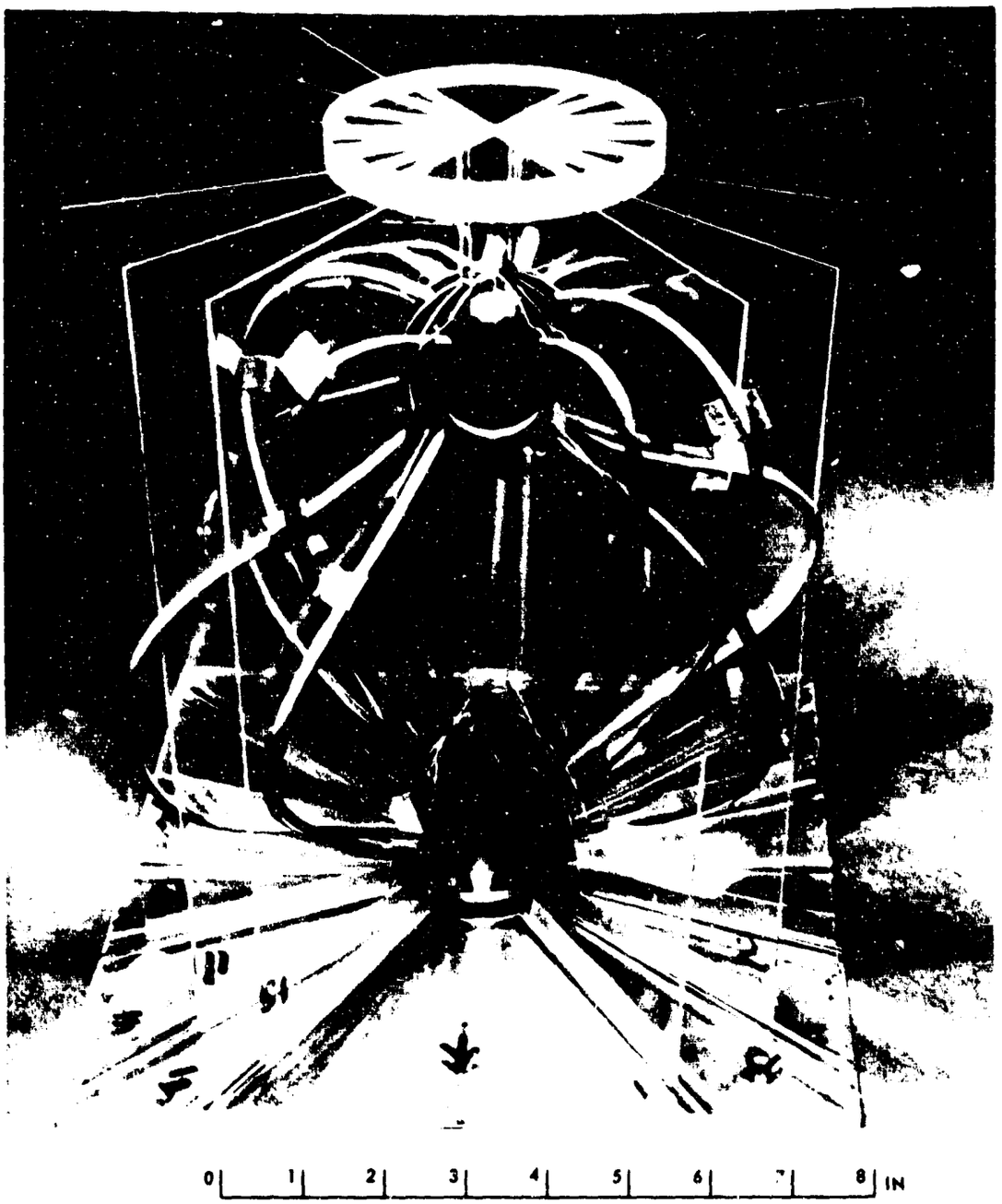

Fig. 6 MOCKUP OF SPHERICAL FOCUSED BLAST DEVICE

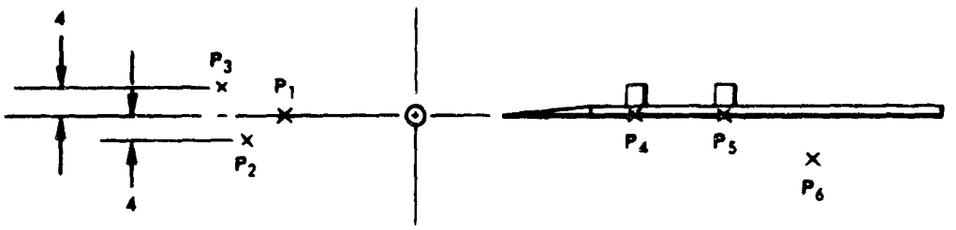

PLAN VIEW

ALL DIMENSIONS IN INCHES

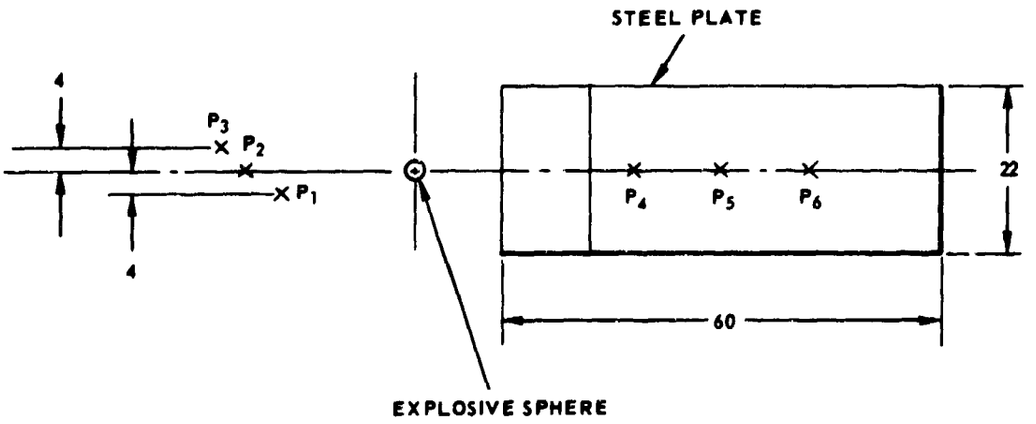

ELEVATION VIEW

Fig. 7 LOCATION OF PRESSURE AND TIME-OF-ARRIVAL GAUGES FOR TEST 3

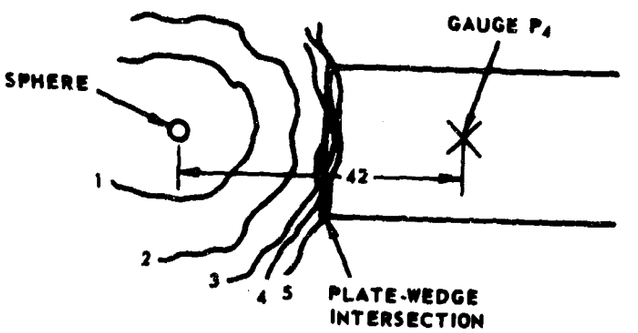

SPHERE 1, FASTAX SPEED = 7171 FRAMES/SECOND

ALL DIMENSIONS IN INCHES

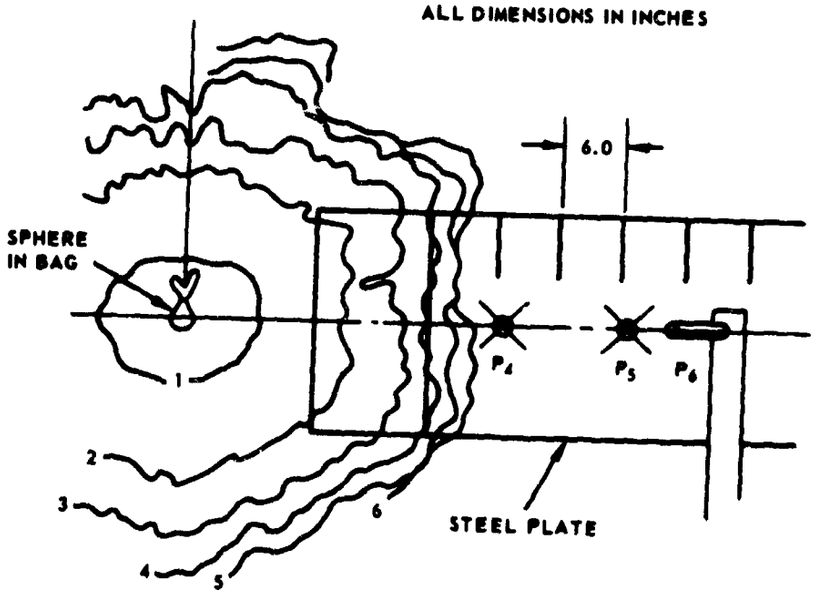

SPHERE 2, FASTAX SPEED = 7271 FRAMES/SECOND

Fig. 8 EXPLOSION PRODUCTS' ENVELOPES FROM CENTRALLY INITIATED SPHERES

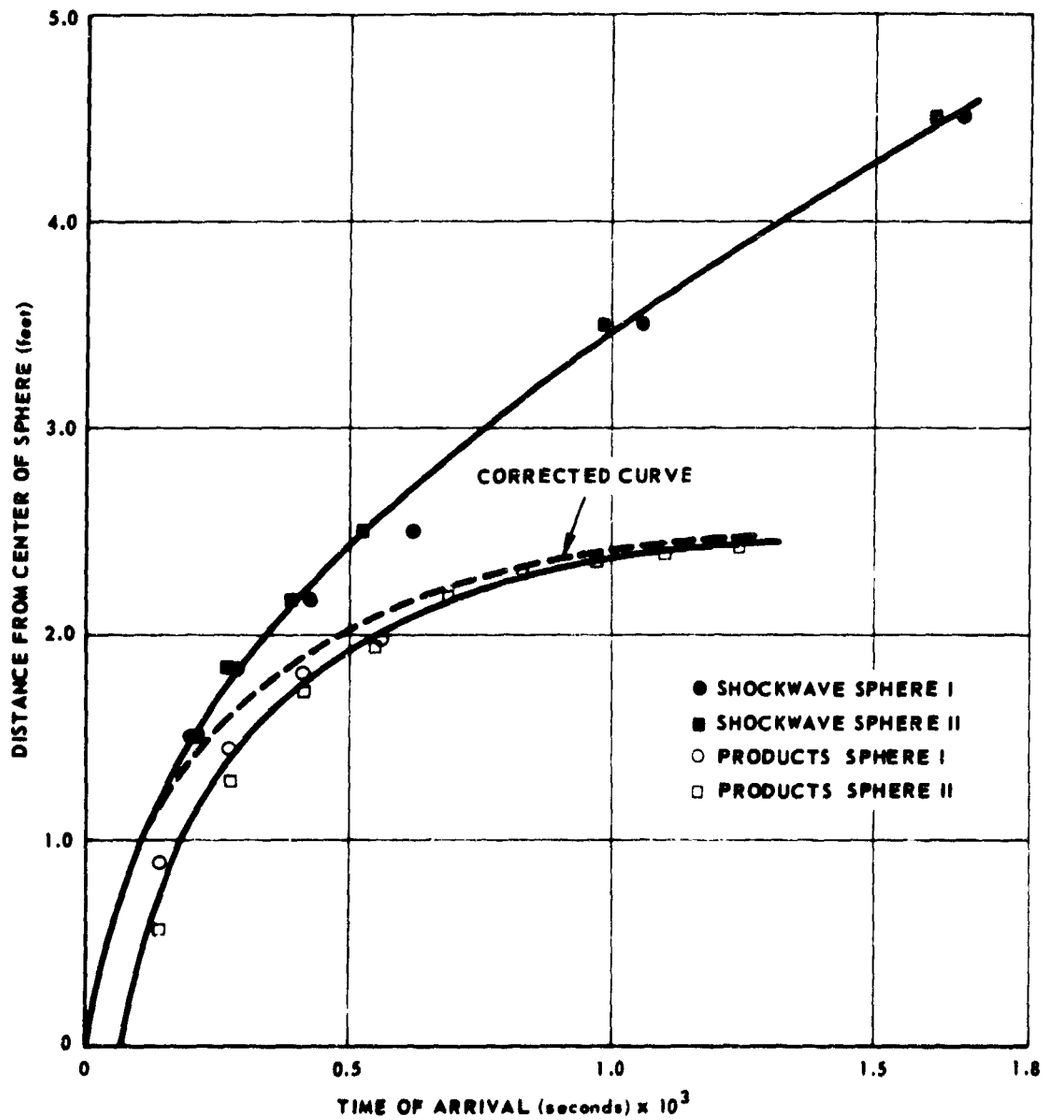

Fig. 9 DISTANCE VERSUS TIME FOR EXPLOSION PRODUCTS AND SHOCKWAVE FROM CENTRALLY INITIATED SPHERES

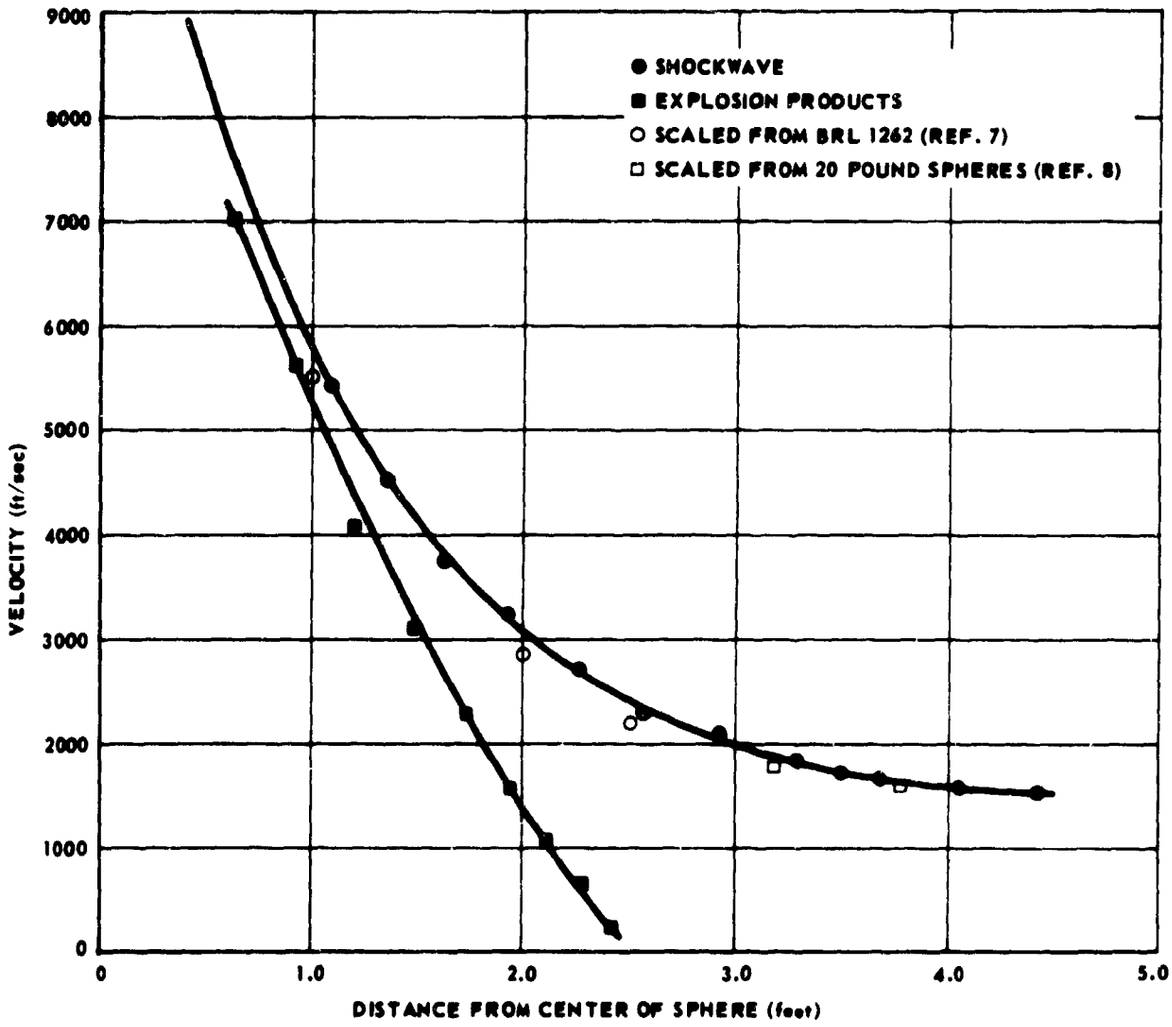

Fig. 10 SHOCKWAVE AND EXPLOSION PRODUCTS' VELOCITIES AS FUNCTIONS OF DISTANCE, FOR CENTRALLY INITIATED SPHERES

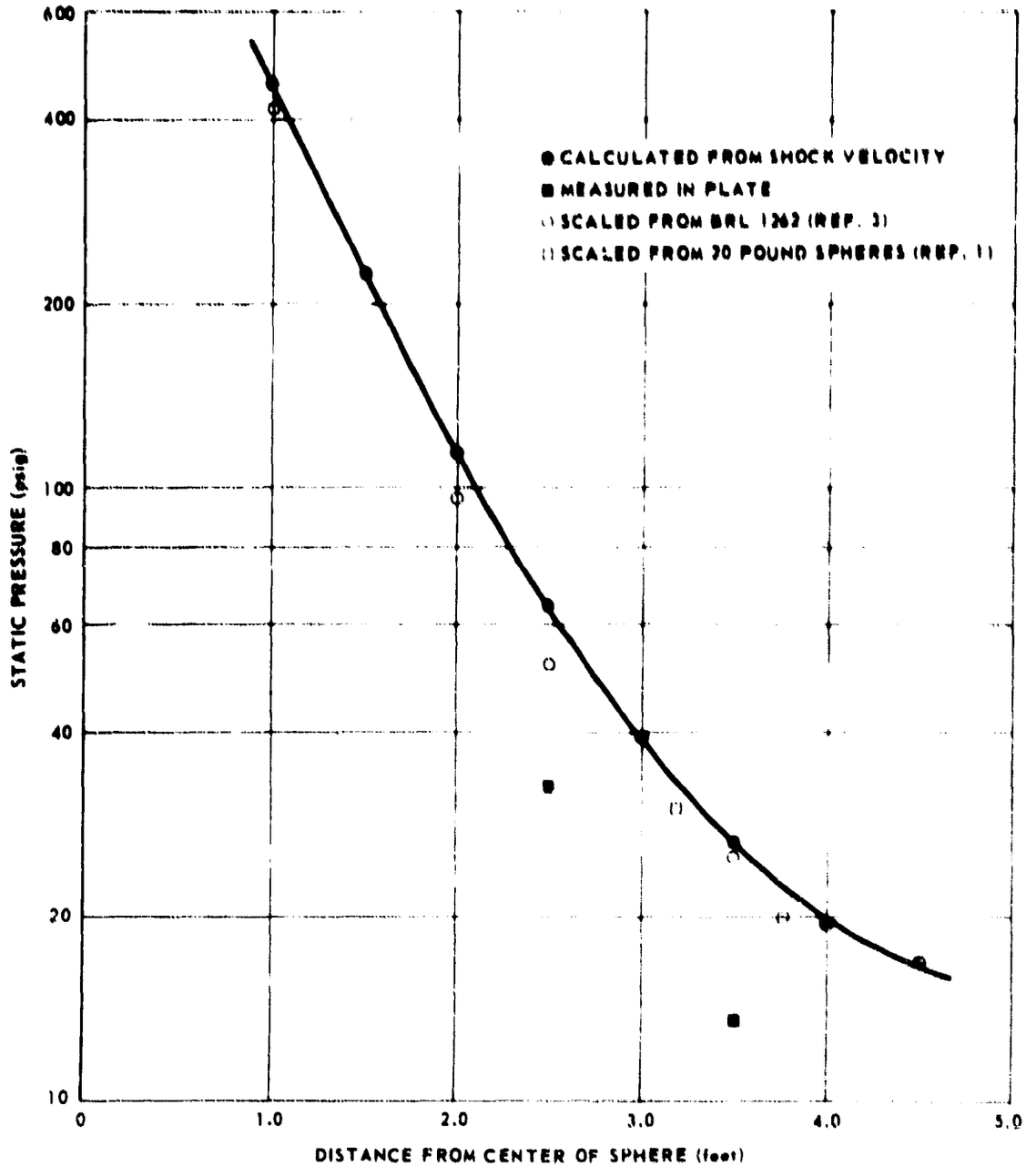

Fig. 11 PEAK OVERPRESSURE AS A FUNCTION OF DISTANCE, FOR CENTRALLY INITIATED SPHERES

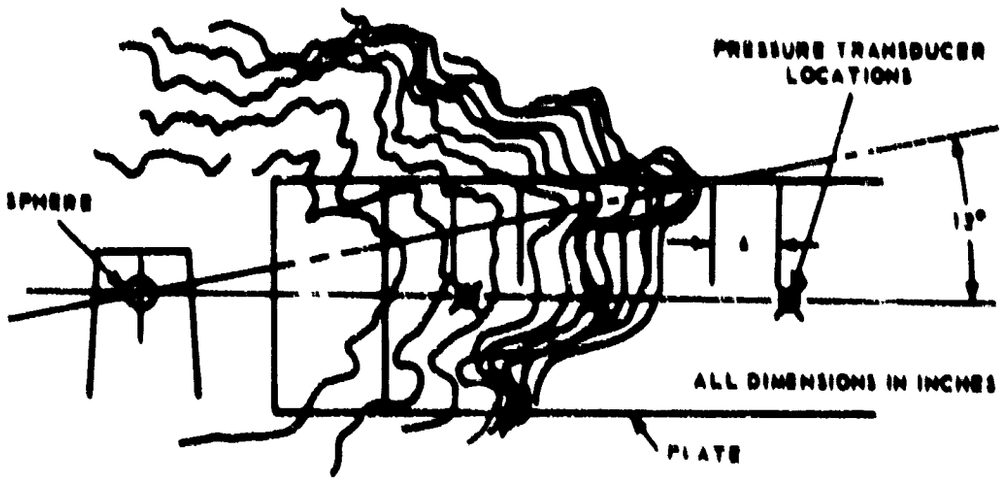

PASTAX SPEED = 7570 FRAMES SECOND

TEST 3

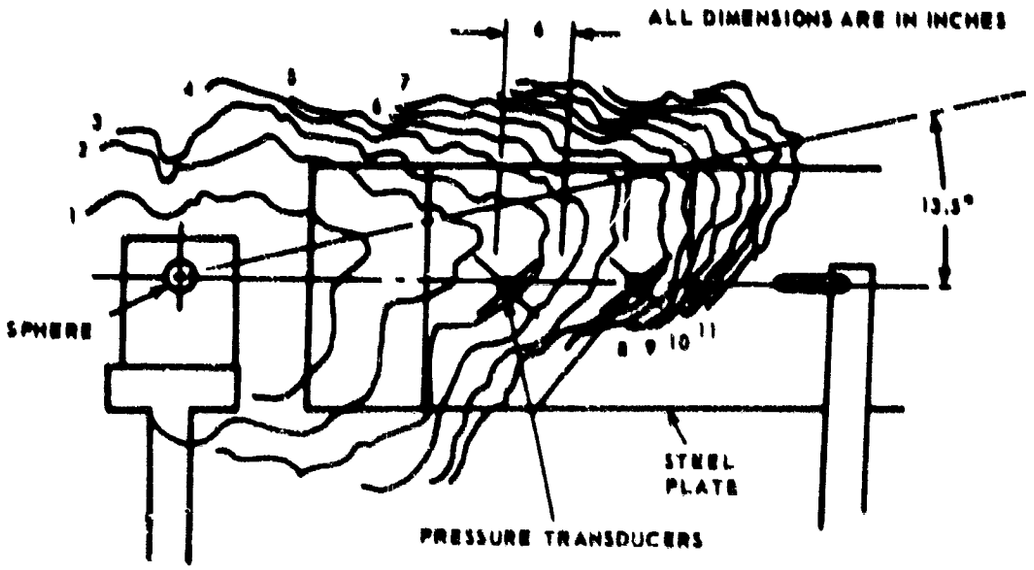

PASTAX SPEED = 7271 FRAMES SECOND

TEST 3

Fig. 12 EXPLOSION PRODUCTS' ENVELOPES FROM THE SECOND AND THIRD TESTS OF THE SPHERICAL FOCUSED BLAST DEVICE

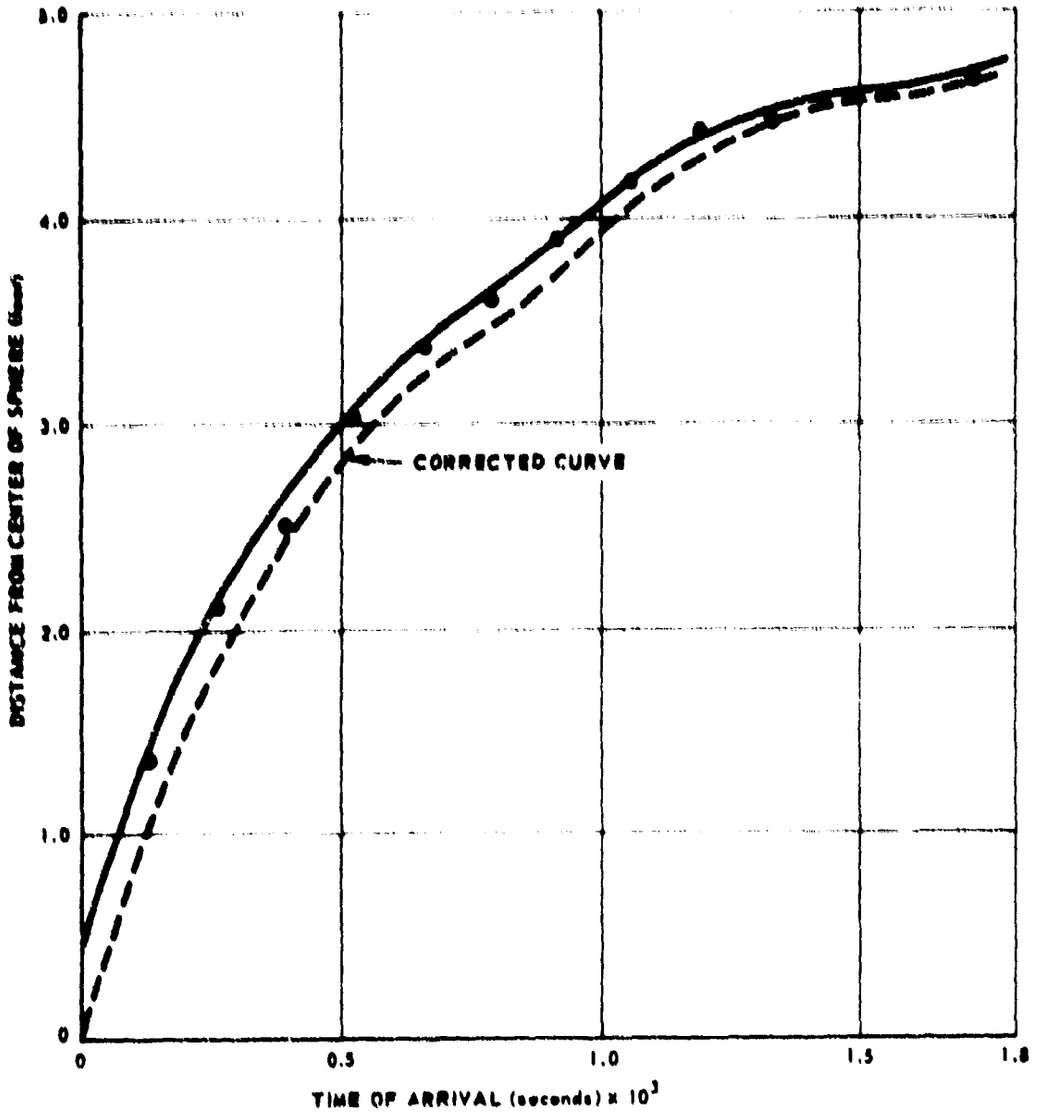

Fig. 13 DISTANCE VERSUS TIME FOR EXPLOSION PRODUCTS FROM SECOND SPHERICAL FOCUSED BLAST DEVICE TEST

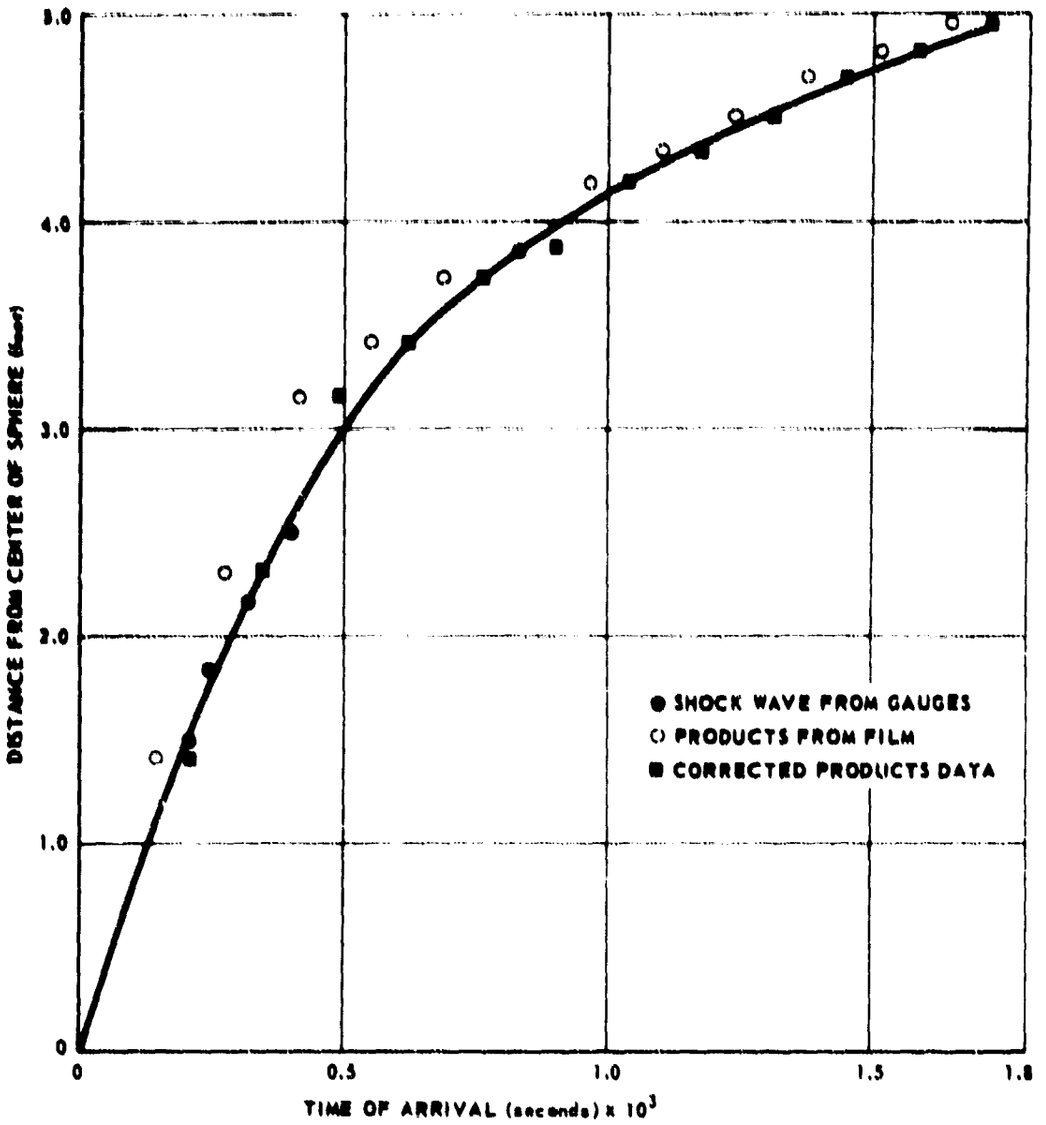

Fig. 14 DISTANCE VERSUS TIME FOR EXPLOSION PRODUCTS AND SHOCKWAVE FROM THIRD SPHERICAL FOCUSED BLAST DEVICE TEST

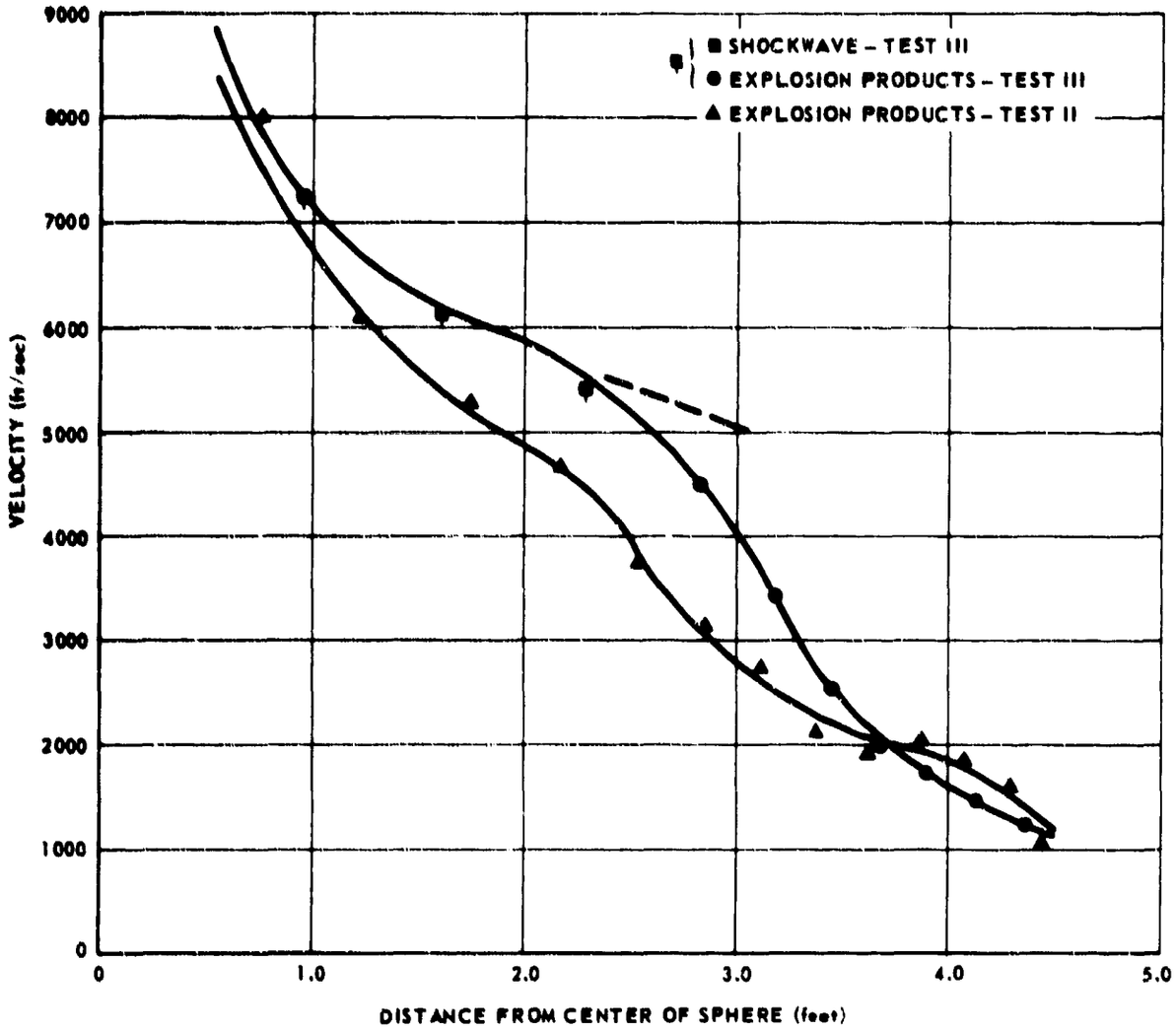

Fig. 15 SHOCKWAVE AND EXPLOSION PRODUCTS' VELOCITIES AS FUNCTIONS OF DISTANCE FOR THE SECOND AND THIRD SHERICAL FOCUSED BLAST DEVICE TESTS

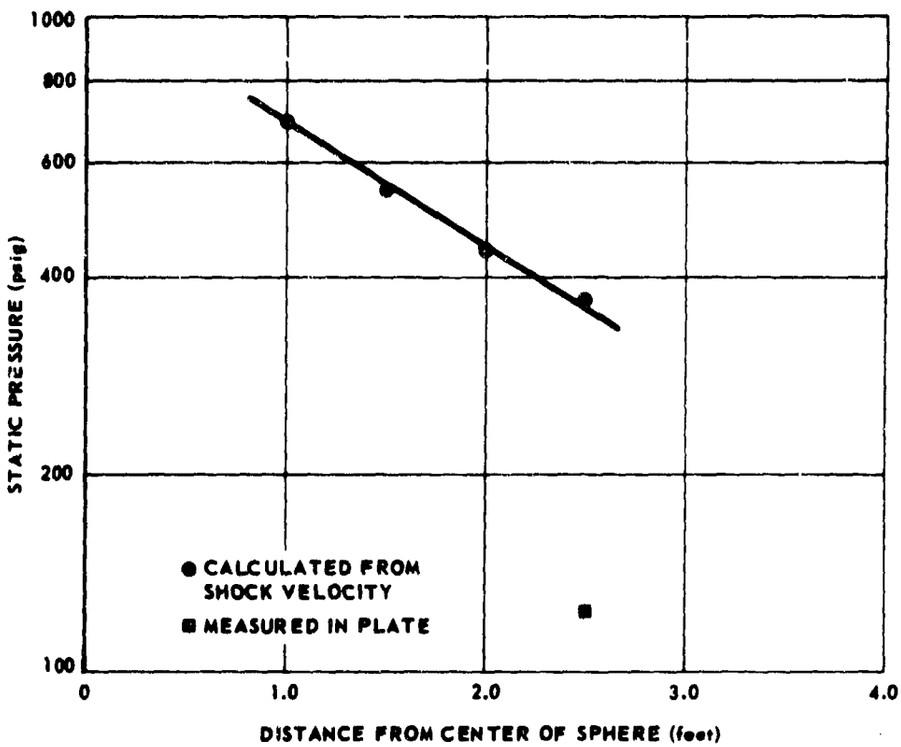

Fig. 16 PEAK OVERPRESSURE AS A FUNCTION OF DISTANCE FOR THE THIRD SPHERICAL FOCUSED BLAST DEVICE TEST

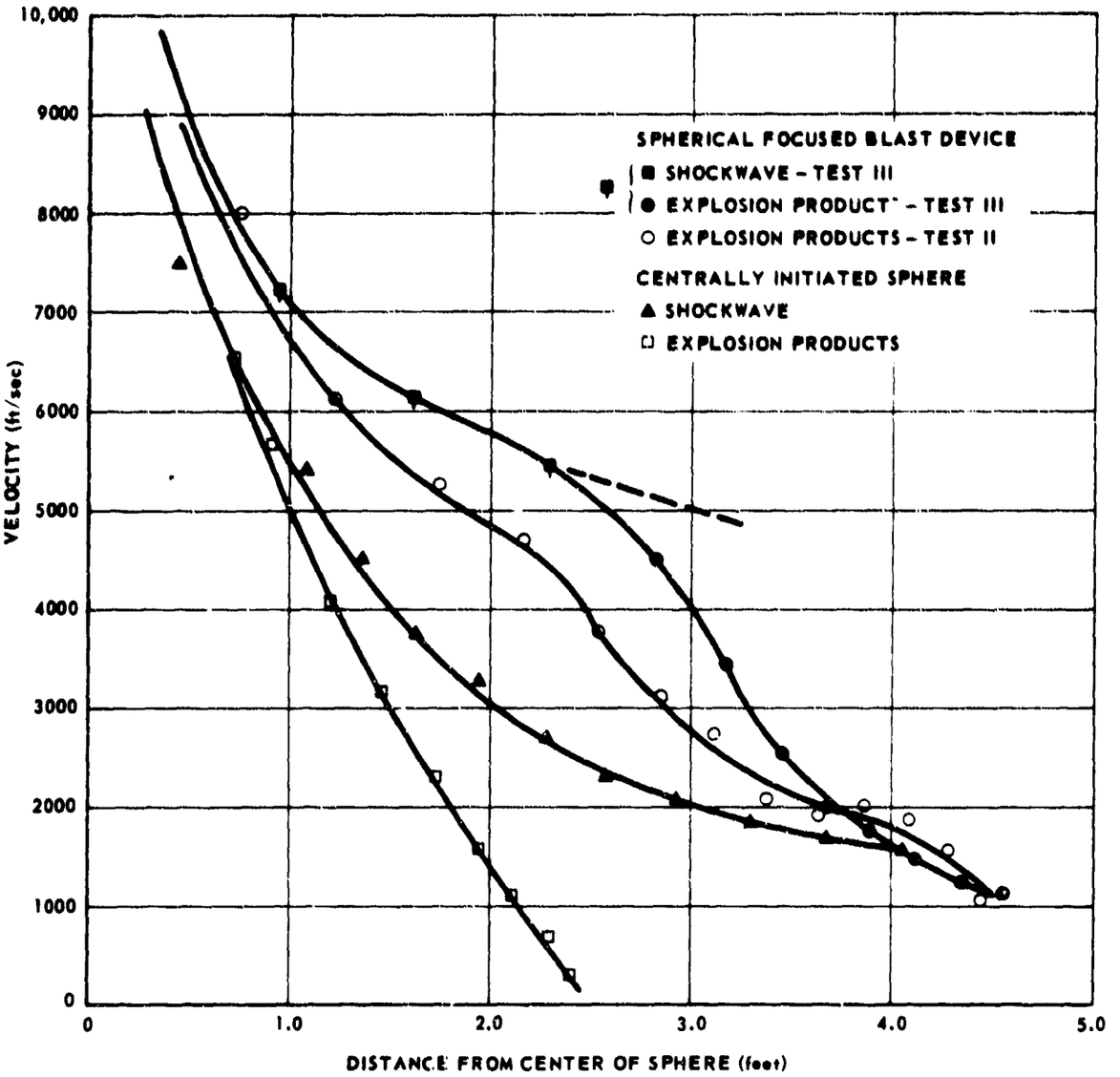

Fig. 17 COMPARISON OF SHOCKWAVE AND EXPLOSION PRODUCTS' VELOCITIES FROM THE SPHERICAL FOCUSED BLAST DEVICE AND CENTRALLY INITIATED SPHERES

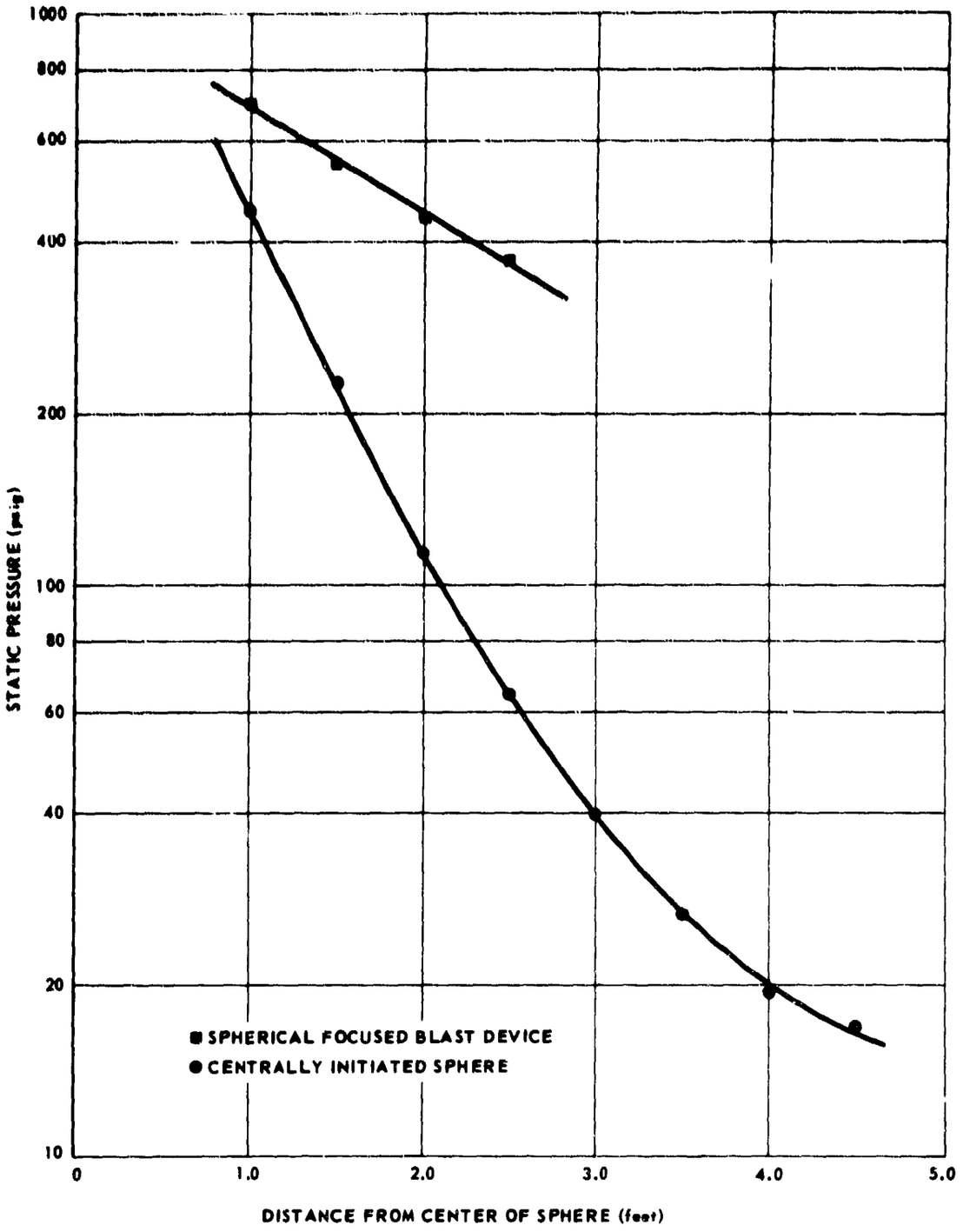

Fig. 18 COMPARISON OF PEAK OVERPRESSURES FROM THE SPHERICAL FOCUSED BLAST DEVICE AND CENTRALLY INITIATED SPHERES

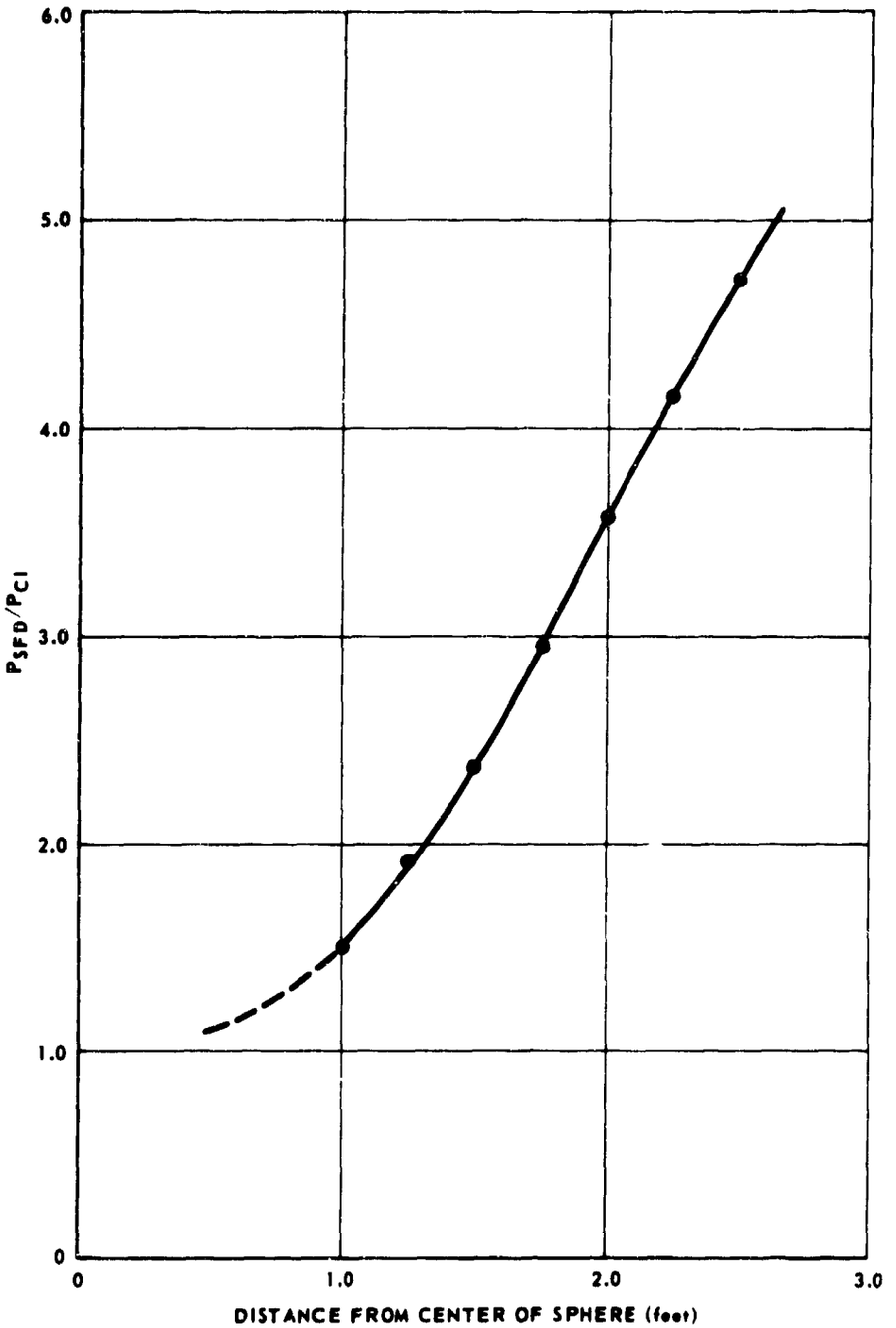

Fig. 19 RATIO OF THE PEAK PRESSURE FROM THE SPHERICAL FOCUSED BLAST DEVICE TO THAT FROM A CENTRALLY INITIATED SPHERE AS A FUNCTION OF DISTANCE

▲ 20 LB DISC, PERIPHERALLY INITIATED
■ 20 LB CONVEX-CONCAVE DISC, PERIPHERALLY INIT.
◆ 20 LB DOUBLE CONVEX DISC, PERIPHERALLY INIT.
● 20 LB SPHERE, MULTIPOINT SIDE INIT.
△ 20 LB SPHERE, CENTRALLY INIT.
□ 60 LB UNCONFINED CYLINDER, SIMULTANEOUS END INIT.
◇ 60 LB CONFINED CYLINDER, SIMULTANEOUS END INIT.
— PENTOLITE DATA OF BRL REP. 1262, 20 LB SPHERE CHARGE USED
○ SPHERICAL FOCUSED BLAST DEVICE (1/4 LB)

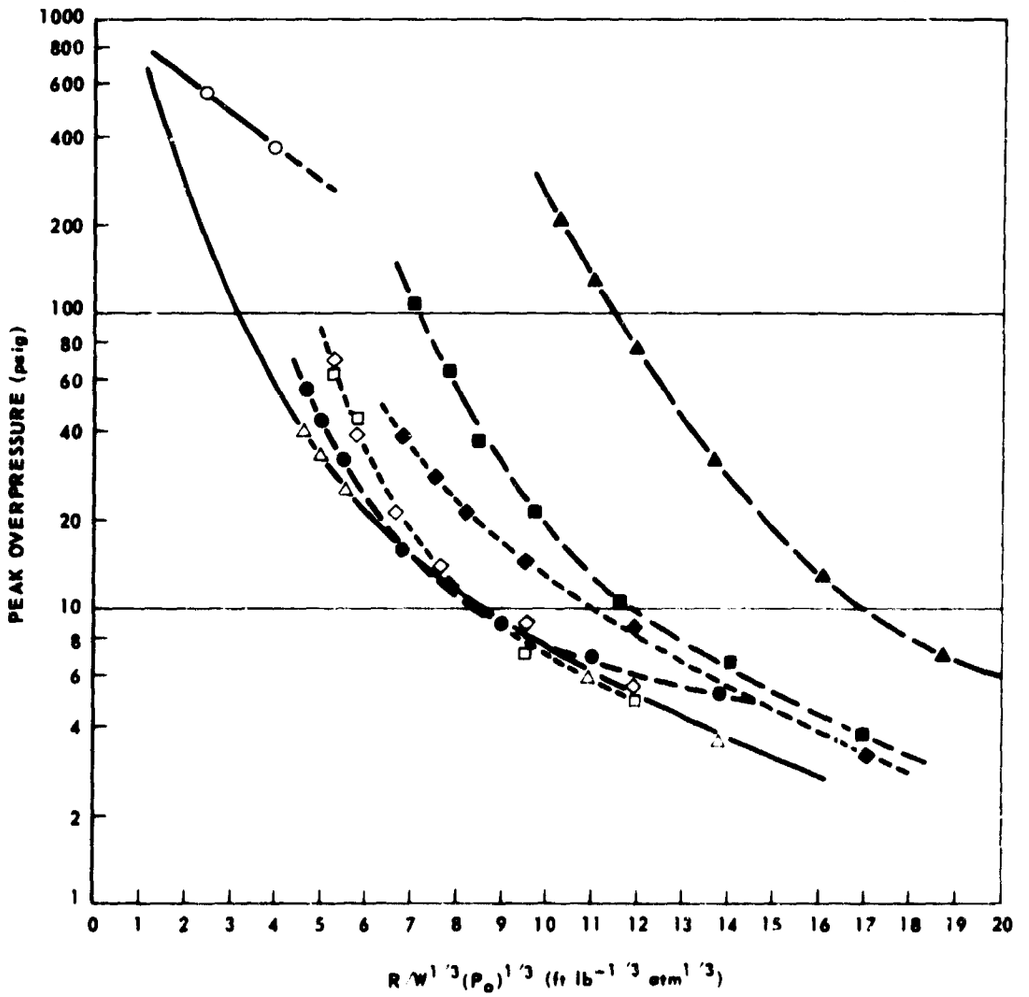

Fig. 20 COMPARISON OF PEAK OVERPRESSURES PRODUCED BY VARIOUS TYPES OF FOCUSED BLAST CHARGES

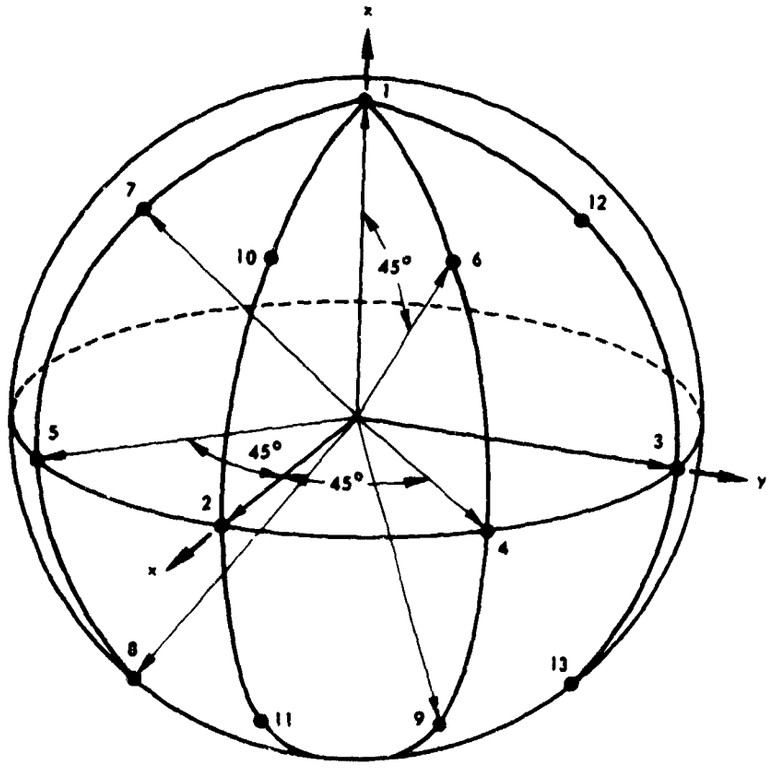

Fig. 21 FIRING AXES FOR A MULTIDIRECTIONAL SPHERICAL FOCUSED BLAST DEVICE

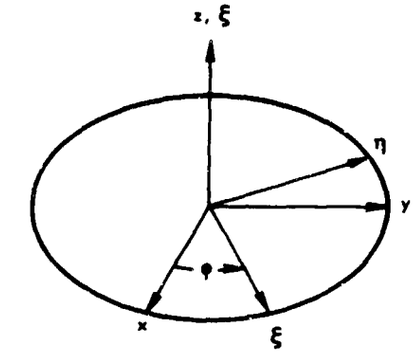

(1)

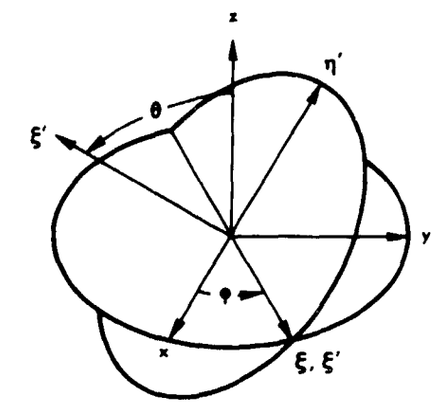

(2)

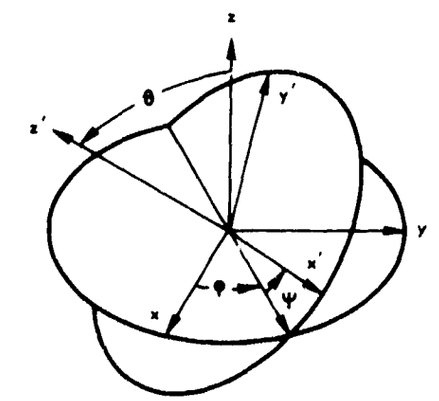

(3)

Fig. 22 COORDINATE ROTATION BY MEANS OF EULER ANGLES

TABLE I

Explosive Weights (grams)

TEST	C-4 SPHERE	DETACORD*	DETASHEET DISK
1	113.6	88.2	7.0
2	116.0	87.2	7.2
3	115.5	87.5	7.0
Centrally Initiated Spheres			
1	115.8	-	-
2	115.8	-	-

* DETACORD LENGTHS:

Long 304.8 mm.

Short 297.8 mm.

TABLE II

Transducer Locations for Centrally Initiated Sphere Tests and the Third Spherical Focused Blast Test.

Number	P_1	P_2	P_3	P_4^*	P_5^*	P_6
Distance from Center of Sphere	18"	22"	26"	30"	42"	46"
Type	∇(1) Atlantic Res. LC-70 ∇(2) Kistler 605B	LC-70	LC-70	(1) 605B (2) LC-70	Kistler 601 L	LC-70

* These transducers are mounted in the steel plate.

∇Transducers at locations P_1 and P_4 were interchanged between the first and second centrally initiated sphere firing. The second arrangement was also used for the third test of the spherical focused blast device.

****

TABLE III

Measured Pressures for Centrally Initiated Sphere Tests

TEST	LOCATION	OVERPRESSURE (psi)
1	P_4 (2.5')	-
1	P_5 (3.5')	14.2
2	P_4 (2.5')	32.2
2	P_5 (3.5')	12.9

TABLE IV

Transducer Locations for Second Spherical Focused Blast Test

Number	P_1	P_2	P_3
Distance from Center of Sphere	30"	42"	60"
Type	Kistler 605B	Kistler 601L	Atlantic Research LC-70

****

TABLE V

Explosive Parameters
(Refs. 3 and 4)

EXPLOSIVE	ADIABATIC EXPONENT γ	ENERGY OF DETONATION $E \left[\frac{cal}{gm}\right]$	DETONATION VELOCITY $D \left[mm/\mu\ s\right]$
C-4	-	-	8.04
RDX	2.736	1228	8.184
50/50 PENTOLITE	2.682	1104	7.465
COMP-B	2.742	1120	7.814

TABLE VI

Values of the Euler Angles for the Firing Axes

FIRING AXIS	φ (rad)	θ (rad)	ψ (rad)
1	0	0	0
2	$\pi/2$	$\pi/2$	0
3	0	$3\pi/2$	0
4	$3\pi/4$	$\pi/2$	0
5	$\pi/4$	$\pi/2$	0
6	$3\pi/4$	$\pi/4$	0
7	$\pi/4$	$\pi/4$	0
8	$\pi/4$	$3\pi/4$	0
9	$3\pi/4$	$3\pi/4$	0

TABLE VII

Transformation Matrices for the Fixing Axes

Axis	A^T
1	$\begin{pmatrix} 1 & 0 & 0 \\ 0 & 1 & 0 \\ 0 & 0 & 1 \end{pmatrix}$
2	$\begin{pmatrix} 0 & 0 & 1 \\ 1 & 0 & 0 \\ 0 & 1 & 0 \end{pmatrix}$
3	$\begin{pmatrix} 1 & 0 & 0 \\ 0 & 0 & 1 \\ 0 & -1 & 0 \end{pmatrix}$
4	$\begin{pmatrix} -\frac{\sqrt{2}}{2} & 0 & \frac{\sqrt{2}}{2} \\ \frac{\sqrt{2}}{2} & 0 & \frac{\sqrt{2}}{2} \\ 0 & 1 & 0 \end{pmatrix}$
5	$\begin{pmatrix} \frac{\sqrt{2}}{2} & 0 & \frac{\sqrt{2}}{2} \\ \frac{\sqrt{2}}{2} & 0 & -\frac{\sqrt{2}}{2} \\ 0 & 1 & 0 \end{pmatrix}$
6	$\begin{pmatrix} -\frac{\sqrt{2}}{2} & -\frac{1}{2} & \frac{1}{2} \\ \frac{\sqrt{2}}{2} & -\frac{1}{2} & \frac{1}{2} \\ 0 & \frac{\sqrt{2}}{2} & \frac{\sqrt{2}}{2} \end{pmatrix}$
7	$\begin{pmatrix} \frac{\sqrt{2}}{2} & -\frac{1}{2} & \frac{1}{2} \\ \frac{\sqrt{2}}{2} & \frac{1}{2} & -\frac{1}{2} \\ 0 & \frac{\sqrt{2}}{2} & \frac{\sqrt{2}}{2} \end{pmatrix}$
8	$\begin{pmatrix} \frac{\sqrt{2}}{2} & \frac{1}{2} & \frac{1}{2} \\ \frac{\sqrt{2}}{2} & -\frac{1}{2} & -\frac{1}{2} \\ 0 & \frac{\sqrt{2}}{2} & -\frac{\sqrt{2}}{2} \end{pmatrix}$
9	$\begin{pmatrix} \frac{\sqrt{2}}{2} & \frac{1}{2} & \frac{1}{2} \\ \frac{\sqrt{2}}{2} & \frac{1}{2} & \frac{1}{2} \\ 0 & \frac{\sqrt{2}}{2} & -\frac{\sqrt{2}}{2} \end{pmatrix}$

TABLE VIII

Location of the Initiation Points * ∇

POINTS	COORDINATES	POINTS	COORDINATES
1 - 1'	$\pm a \begin{pmatrix} 0 \\ 0 \\ 1 \end{pmatrix}$	10 - 10'	$\pm \frac{a\sqrt{2}}{2} \begin{pmatrix} 1 \\ 0 \\ 1 \end{pmatrix}$
2 - 2'	$\pm a \begin{pmatrix} 1 \\ 0 \\ 0 \end{pmatrix}$	11 - 11'	$\pm \frac{a\sqrt{2}}{2} \begin{pmatrix} 1 \\ 0 \\ -1 \end{pmatrix}$
3 - 3'	$\pm a \begin{pmatrix} 0 \\ 1 \\ 0 \end{pmatrix}$	12 - 12'	$\pm \frac{a\sqrt{2}}{2} \begin{pmatrix} 0 \\ 1 \\ 1 \end{pmatrix}$
4 - 4'	$\pm \frac{a\sqrt{2}}{2} \begin{pmatrix} 1 \\ 1 \\ 0 \end{pmatrix}$	13 - 13'	$\pm \frac{a\sqrt{2}}{2} \begin{pmatrix} 0 \\ 1 \\ -1 \end{pmatrix}$
5 - 5'	$\pm \frac{a\sqrt{2}}{2} \begin{pmatrix} 1 \\ -1 \\ 0 \end{pmatrix}$	a - a'	$\pm \frac{a\sqrt{2}}{4} \begin{pmatrix} 1 - \sqrt{2} \\ 1 + \sqrt{2} \\ \sqrt{2} \end{pmatrix}$
6 - 6'	$\pm \frac{a}{2} \begin{pmatrix} 1 \\ 1 \\ \sqrt{2} \end{pmatrix}$	b - b'	$\pm \frac{a\sqrt{2}}{4} \begin{pmatrix} 1 + \sqrt{2} \\ 1 - \sqrt{2} \\ \sqrt{2} \end{pmatrix}$
7 - 7'	$\pm \frac{a}{2} \begin{pmatrix} 1 \\ -1 \\ \sqrt{2} \end{pmatrix}$	c - c'	$\pm \frac{a\sqrt{2}}{4} \begin{pmatrix} 1 + \sqrt{2} \\ -1 + \sqrt{2} \\ \sqrt{2} \end{pmatrix}$
8 - 8'	$\pm \frac{a}{2} \begin{pmatrix} 1 \\ -1 \\ -\sqrt{2} \end{pmatrix}$	d - d'	$\pm \frac{a\sqrt{2}}{4} \begin{pmatrix} 1 - \sqrt{2} \\ -1 - \sqrt{2} \\ \sqrt{2} \end{pmatrix}$
9 - 9'	$\pm \frac{a}{2} \begin{pmatrix} 1 \\ 1 \\ -\sqrt{2} \end{pmatrix}$	e - e'	$\pm \frac{a\sqrt{2}}{4} \begin{pmatrix} 1 + \sqrt{2} \\ -1 + \sqrt{2} \\ -\sqrt{2} \end{pmatrix}$

* Numbers refer to points marked in Figure 23.

∇ Primes are associated with the minus (-) sign.

TABLE VIII (Cont'd)

POINTS		COORDINATES
f - f'	$\pm \frac{a\sqrt{2}}{4}$	$\begin{pmatrix} 1 - \sqrt{2} \\ -1 - \sqrt{2} \\ -\sqrt{2} \end{pmatrix}$
g - g'	$\pm \frac{a\sqrt{2}}{4}$	$\begin{pmatrix} 1 - \sqrt{2} \\ 1 + \sqrt{2} \\ -\sqrt{2} \end{pmatrix}$
h - h'	$\pm \frac{a\sqrt{2}}{4}$	$\begin{pmatrix} 1 + \sqrt{2} \\ 1 - \sqrt{2} \\ -\sqrt{2} \end{pmatrix}$

TABLE IX

Firing Order of Initiation Points

Firing Axis	Initiation Time	
	$t = 0$	$t = t_{delay}$
1 - 1'	2 - 2' & 3 - 3'	10 - 10', 11 - 11', 12 - 12' & 13 - 13'
2 - 2'	1 - 1' & 3 - 3'	4 - 4', 5 - 5', 10 - 10' & 11 - 11'
3 - 3'	1 - 1' & 2 - 2'	4 - 4', 5 - 5', 12 - 12' & 13 - 13'
4 - 4'	1 - 1' & 5 - 5'	2 - 2', 3 - 3', 6 - 6' & 9 - 9'
5 - 5'	1 - 1' & 4 - 4'	2 - 2', 3 - 3', 7 - 7' & 8 - 8'
6 - 6'	5 - 5' & 9 - 9'	a - a', b - b', 1 - 1' & 4 - 4'
7 - 7'	4 - 4' & 8 - 8'	c - c', d - d', 1 - 1' & 5 - 5'
8 - 8'	4 - 4' & 7 - 7'	e - e', f - f', 1 - 1' & 5 - 5'
9 - 9'	5 - 5' & 6 - 6'	g - g', h - h', 1 - 1' & 4 - 4'

References

1. D.K. Parks and G.S. Weeding, "Investigation of Characteristics Around Focused Blast Charges," Falcon Research and Development Company Contract Report, APL/JHU BFM-043, March 1967.
2. S. Feldman, "Hypersonic Gas Dynamics Charts for Equilibrium Air," AVCO Res. Lab., 1957.
3. R.E. Shear, "Incident and Reflected Blast Pressures for Pentolite," BRL 1262, September 1964.
4. D. Price, private communication, 1959 (via H. Sternberg NOL/WO).
5. D. Price, Chem. Revs., 59, 801, 1959.
6. H. Goldstein, Classical Mechanics, Addison-Wesley, 1956, Chapt. 4.

INITIAL DISTRIBUTION EXTERNAL TO THE APPLIED PHYSICS LABORATORY*

The work reported in TG-1001 was done under Navy Contract NOw 62-0604-c. This work is related to Task X82, which is supported by the Naval Ordnance Systems Command.

ORGANIZATION	LOCATION	ATTENTION	No. of Copies
DEPARTMENT OF DEFENSE			
DDC	Alexandria, Va.		20
Department of the Navy			
NAVORDSYSCOM	Washington, D. C.	ORD 03521	2
		ORD 9132	2
NAVAIRSYSCOM	Washington, D. C.	AIR 350	2
		AIR 604	2
Naval Weapons Center	China Lake, Calif.	P. Cordle, Code 456	1
NAVPLANTREPO/SS	Silver Spring, Md.		1

Requests for copies of this report from DoD activities and contractors should be directed to DDC, Cameron Station, Alexandria, Virginia 22314 using DDC Form 1 and, if necessary, DDC Form 55.

*Initial distribution of this document within the Applied Physics Laboratory has been made in accordance with a list on file in the APL Technical Reports Group.

UNCLASSIFIED
Security Classification

DOCUMENT CONTROL DATA - R & D

(Security classification of title, body of abstract and indexing annotation must be entered when the overall report is classified)

1. ORIGINATING ACTIVITY *(Corporate author)*
The Johns Hopkins Univ. Applied Physics Lab.
8621 Georgia Ave.
Silver Spring, Maryland 20910

2a. REPORT SECURITY CLASSIFICATION
Unclassified

2b. GROUP

3. REPORT TITLE
A Spherical Focused Blast Device

4. DESCRIPTIVE NOTES *(Type of report and inclusive dates)*

5. AUTHOR(S) *(First name, middle initial, last name)*
Russell L. McCally

6. REPORT DATE	7a. TOTAL NO. OF PAGES	7b. NO. OF REFS
May 1968	60	6

8a. CONTRACT OR GRANT NO.	9a. ORIGINATOR'S REPORT NUMBER(S)
NOw 62-0604-c	TG-1001
b. PROJECT NO.	
c.	9b. OTHER REPORT NO(S) *(Any other numbers that may be assigned this report)*
d.	

10. DISTRIBUTION STATEMENT
This document has been approved for public release and sale; its distribution is unlimited.

11. SUPPLEMENTARY NOTES	12. SPONSORING MILITARY ACTIVITY
	Naval Ordnance Systems Command

13. ABSTRACT

A spherical explosive device that, by selective multipoint initiation, concentrates its energy in a beam along any of several aiming axes is described. Aiming is accomplished by electronically selecting the proper group of detonators, thereby eliminating the necessity of physically aiming the charge as is required in all other focused blast devices. Once fired, these initiators cause a nearly cylindrical detonation wave, collapsing on the focusing axis, which forces the explosive products out along this axis. Three small 1/4 lb. C-4 spherical focused blast devices have been built and fired. The explosion products' velocity, shock wave velocity and peak pressure along the focusing axis were measured. These blast parameters were compared with similar ones measured for centrally initiated spheres, the purpose being to achieve a quantitative measure of the degree of focusing. The comparisons revealed that considerable gains over isotropic blast result from this focusing method. Furthermore the focusing appears to be a far field effect in that the values of peak pressure and the shock velocity are nearly equal to those of the centrally initiated sphere in close but tend to fall off much less rapidly with distance. Another result of interest is that the data obtained from the small, 1/4 lb., 2 inch diameter, centrally initiated spheres are in very good agreement with similar data scaled from much larger spheres.

DD FORM 1 NOV 68 1473

UNCLASSIFIED
Security Classification

14.	KEY WORDS

Focused blast
Blast effects
Multipoint initiation
C-4 explosive